Available online at www.sciencedirect.com
SCIENCE DIRECT®
Geochimica et Cosmochimica Acta 70 (2006) 461–479
Geochimica
www.elsevier.com/locate/gca

Trace element degassing and enrichment in the eruptive plume of the 2000 eruption of Hekla volcano, Iceland

Séverine Moune [a,*], Pierre-J. Gauthier [a], Sigurdur R. Gislason [b], Olgeir Sigmarsson [a,b]

[a] *Laboratoire Magmas et Volcans, Observatoire de Physique du Globe de Clermont-Ferrand, CNRS—Université Blaise Pascal—IRD, 5 rue Kessler, 63038 Clermont-Ferrand Cedex, France*
[b] *Institute of Earth Sciences, University of Iceland, Sturlugata 7, 101 Reykjavik, Iceland*

Received 8 March 2005; accepted in revised form 6 September 2005

Abstract

During its last eruption in February 2000, Hekla volcano (Iceland) emitted a sub-Plinian plume that was condensed and scavenged down to the ground by heavy snowstorms, offering the unique opportunity to study the chemistry of the gaseous plume released during highly explosive eruptions. In this paper, we present results on trace element and minor volatile species (sulfates, chlorides, and fluorides) concentrations in snow samples collected shortly after the beginning of the eruption. The goal of this study is to better constrain the degassing and mobility of trace elements in gaseous emissions. Trace element volatility at Hekla is quantified by means of enrichment factors (EF) relative to Be. Well-known volatile trace elements (e.g., transition metals, heavy metals, and metalloids) are considerably enriched in the volcanic plume of Hekla. Their abundances are governed by the primary magmatic degassing of sulfate and/or halide compounds, which are gaseous at magmatic temperature. Their volatility is, however, slightly lower than in basaltic systems, most likely because of the lower magma temperature and higher magma viscosity at Hekla. More surprisingly, refractory elements (e.g., REE, Th, Ba, and Y) are also significantly enriched in the eruptive plume of Hekla where their apparent volatility is two orders of magnitude higher than in mafic systems. In addition, REE patterns normalized to the Hekla 2000 lava composition show a significant enrichment of HREE over LREE, suggesting the presence of REE fluorides in the volcanic plume. Such enrichments in the most refractory elements and REE fractionation are difficult to reconcile with primary degassing processes, since REE fluorides are not gaseous at magma temperature. REE enrichments at Hekla could be attributed to incongruent dissolution of tephra grains at low temperature by F-rich volcanic gases and aerosols within the eruptive plume. This view is supported by both leaching experiments performed on Hekla tephra and thermodynamic considerations on REE mobility in hydrothermal fluids and modeling of glass dissolution in F-rich aqueous solutions. Tephra dissolution may also explain the observed enrichments in other refractory elements (e.g., Th, Y, and Ba) and could contribute to the degassing mass balance of some volatile trace elements, provided they are mobile in F-rich fluids. It thus appears that both primary magmatic degassing and secondary tephra dissolution processes govern the chemistry of eruptive plumes released during explosive eruptions.

1. Introduction

The magmatic gas phase plays a major role at active volcanoes and the interest in studying volcanic gases has been continuously increasing in modern volcanology. First, the dynamics of eruptive processes (explosivity, eruptive style, and intensity) are known to be linked to both gas concentration in magmas and the physics of the degassing process itself (e.g., Jaupart, 1996, 1998). Second, degassing is one of the main and most common manifestations of volcanic activity. Many active volcanoes display a persistent degassing activity, even during quiet periods. Gases, therefore, represent a unique interface between the Earth's surface and magma at depth. Accordingly, numerous studies have recently focused on time-series analyses of gas chemistry at active volcanoes to understand changes in physical and chemical conditions within magma reservoirs. Such information could then be used to both monitor geochemical

* Corresponding author. Fax: +33 4 73 34 67 44.
E-mail address: S.Moune@opgc.univ-bpclermont.fr (S. Moune).

0016-7037/$ - see front matter © 2005 Elsevier Inc. All rights reserved.
doi:10.1016/j.gca.2005.09.011

precursors before an eruption and better constrain the evolution of active magmatic systems (e.g., Symonds et al., 1994; Goff et al., 1998; Allard et al., 2005 and references therein).

In addition, volcanic emissions contribute to the natural atmospheric cycles of many gas species and trace elements (e.g., Aiuppa et al., 2003). Beside major (H_2O, CO_2, SO_2, H_2S, HCl, HF, etc.) and minor (N_2, rare gases, CO, CH_4, H_2, etc.) components, it is indeed well known since the early work by Zoller et al. (1974) that volcanic gases and aerosols are considerably enriched in many trace elements including alkali, alkali-earth, transition, and heavy metals. Such trace element enrichments are always observed in gaseous emanations from volcanoes worldwide, provided that magma temperature is high enough to ensure their volatilization (e.g., Le Guern, 1988; Symonds et al., 1994; Delmelle and Stix, 2000 and references therein). Volcanic gas emissions may modify the chemical composition of the atmosphere at the local scale and, for larger eruptions, may affect global climate and alter the Earth's radiation budget, notably for greenhouse gases (CO_2) and sulfur species (e.g., Rampino and Self, 1992; Thordarson et al., 2001). However, apart from cataclysmal eruptions, volcanic gases and aerosols released during moderate eruptions and/or quiescent degassing usually appear to be negligible compared to anthropogenic pollution (Nriagu, 1989). Nonetheless, for some trace elements, this volcanic input may have a significant impact on the local environment by either polluting (e.g., toxic heavy metals) or fertilizing (e.g., alkali and alkali-earth metals) terrestrial and aquatic ecosystems (Frogner et al., 2001). It is thus of primary importance to assess trace element fluxes released into the atmosphere by volcanic activity.

While most of previous studies dealt with trace element fluxes released during quiescent degassing or moderate eruptive activity, we present here data on the volatility of trace elements released during a sub-Plinian eruption at Hekla volcano, Iceland. This paper focuses on the chemical composition of the early sub-Plinian phase of the 2000 eruption that was trapped and scavenged down to the ground by heavy snowstorms soon after its emission. These snow samples yield a unique opportunity to study the chemistry of gases and volcanic aerosols emitted during such explosive eruptions, which is otherwise inaccessible for obvious safety reasons.

The aim of this study was to better constrain the degassing and mobility of trace elements in tephra-gaseous plumes released during explosive eruptions, taking into account the influence of both magma temperature and composition, as well as that of the major gases. We will show in this paper that well-known volatile trace elements (e.g., alkalis, heavy metals, and transition metals) are degassed in the plume of Hekla, as previously observed at mafic volcanoes. More surprisingly, refractory elements including rare earth elements (REE) are also significantly enriched in the plume of Hekla. Theoretical considerations as well as laboratory experiments on tephra dissolution in a F-rich fluid are presented to explain the occurrence of these refractory elements in snow samples.

2. Sampling and analytical procedures

2.1. Sampling sites, sampling procedures, and sample preparation

Hekla volcano (63.98°N, 19.70°W; 1491 m a.s.l.) is located in the southern part of Iceland at the intersection of the South Iceland Fracture Zone with the South Iceland Volcanic Zone and is built up on a WSW-ENE trending fissure (Fig. 1). The last eruption of Hekla started on February 26, 2000 at 6:19 pm GMT. Initially, a 5-km-long eruptive fissure opened on the crest and along the southeastern flank of the Hekla ridge. A sub-Plinian eruptive column rose up from the summit crater on the fissure and reached a height of about 11 km a few minutes later, before being carried northwards by light winds following a main azimuth at N25°E (Fig. 1). From 9.00 pm, wind direction slightly shifted westwards reaching a main azimuth at about N5°W at 1.00 am on February 27. These azimuths are those of the volcanic plume at heights above 7–8 km and may differ from the azimuth of tephra deposition (which was N15°E during the first hours of the eruption), suggesting that low-level winds into which falling particles were advected on their way to the ground had a slightly different direction (Lacasse et al., 2004). Further details on both the eruptive sequence and local weather conditions may be found in Lacasse et al. (2004 and references therein).

Continuous heavy snow showers were recorded on February 26 and 27, and fell through the volcanic plume, condensing and scavenging it down to the ground. Fresh snow samples were collected on the ground 18–23 h after the beginning of the eruption at sampling sites located 10–20 km north of Hekla (Fig. 1). The presence of tephra in snow layers constrained whether the snow layers fell during, before, or after the early hours of the eruption (Fig. 2). The mixture of tephra and snow was sampled into heavy walled 30-liter plastic bags, which had been washed with 0.1 M hydrochloric acid for more than an hour, and then carefully rinsed several times with DI-water. At each sampling site about 1 m^2 was cleared of the first few centimeters of snow that fell after the deposition of the sub-Plinian unit. This was done gently with a glove-covered hand using a new set of disposable powder free Latex surgical gloves at each site. The few-centimeter thick layer of tephra and snow corresponding to the sub-Plinian phase of the eruption was then sampled (Fig. 2). Sampling bags were finally carefully closed to avoid any contamination and packed into insulation boxes, which were half filled with snow to ensure no melting of the snow samples during their transport to the laboratory.

Samples were kept in a freezer at −18 °C until they were melted by immersing the plastic bags into hot water (60–95 °C) in the laboratory sink for 30 min. Once all snow

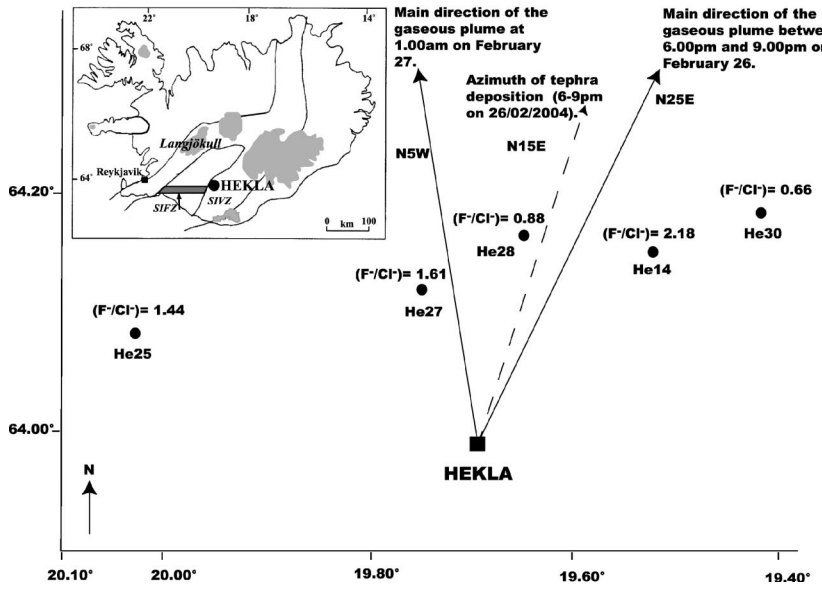

Fig. 1. Localization of the sampling sites in the vicinity of Hekla volcano, Iceland. Coordinates determined with a GPS are: He14 (64.15°N–19.52°W), He25 (64.08°N–20.02°W), He27 (64.12°N–19.75°W), He28 (64.16°N–19.65°W), and He30 (64.18°N–19.42°W). Also shown are the main azimuths of both plume propagation and tephra deposition during the first two days of the February 2000 eruption (Lacasse et al., 2004). Inset: simplified sketch map of Iceland showing Hekla volcano at the intersection of the South Iceland Fracture Zone (in gray; SIFZ) with the South Iceland Volcanic Zone (SIVZ). Also reported are the main glaciers of Iceland including Langjökull, a glacier northwest of Hekla where sample L2 (atmospheric background) was collected.

Fig. 2. Photograph of a tephra-snow layer collected during the course of this study. The thickness of the tephra layer corresponding to the sub-Plinian phase is approximately 2.5 cm.

was melted, conductivity and pH of the solutions were measured in a small sampling bottle at room temperature. To eliminate tephra and solid particles, solutions were immediately filtered through 0.2 μm cellulose acetate filters (142-mm diameter) held in a Teflon filter-holder (Sartorius) washed in 0.1 M analytical grade HCl and thoroughly rinsed with DI-water. The first liter of each solution was used to "pre-contaminate" the filter—filter-holder—tubing and was subsequently discarded. Filtrated solutions were then pumped by a peristaltic pump into polyethylene bottles. Bottles for metal and nutrient analysis were acid-washed by 0.1 M HCl and thoroughly cleaned with DI-water. All sample bottles were also "pre-contaminated" with the filtrated samples. One milliliter of suprapure HNO_3 was finally added to the 100 ml samples intended for metal analysis.

This study is based on five samples of snow (He14, He25, He27A and B, He28, and He30), that fell through the diluted plume of Hekla and scavenged it down to the ground. Samples He27A and He27B correspond to a single sampling site but stored in two different bottles. Another snow sample (L2) was collected in March 2000 on the Langjökull glacier (Fig. 1; 64.59°–20.34°) using acid and DI-water-washed polycarbonate snow corer. Melting and sample preparation was similar to that used for Hekla snow samples. This sample represents the mass average of the October 1999–March 2000 winter precipitation in the highlands of SW-Iceland out of the influence zone of the eruptive plume. Accordingly, this sample is taken as a reference sample representative of the average chemical composition of atmospheric precipitations in SW Iceland for this period.

A sample of the March 2 lava flow (HK2000L) from the Hekla 2000 eruption as well as tephra erupted during the sub-Plinian phase (HK2000T) collected shortly after their eruption allow the comparison of their chemical compositions with those of the snow samples. The lava flow sample was grounded below 100 μm in a tungsten-carbide grinding mill to obtain a homogeneous powder, representative of the whole rock chemical composition. The tephra sample was crushed below 1 mm in a hardened-steel jaw crusher and the 100–250 μm granulometric fraction was sieved to conduct leaching experiments. This fraction was first cleaned in DI-water and dried at 50 °C in a drying oven.

Rare mineral phases (mostly plagioclase and olivine crystals) were subsequently eliminated using a Frantz magnetic separator to obtain a pure fraction of pristine glass.

2.2. Chemical treatments, instrumentation, and data acquisition

All chemical treatments of snow solution samples and rock powder were carried out using purified (double-Quartex distillation followed by sub-boiling of commercial acids) ultra-pure acids and milli-Q water in a class A clean room.

Rock powder aliquots of about 100 mg were digested in a mixture of concentrated HF–HNO_3–$HClO_4$. After complete digestion, solutions were gently evaporated (~60 °C) until $HClO_4$ began to fume and then evaporated to dryness at higher temperature (120 °C). Solid residues were taken up twice in 7 N HNO_3 to obtain a perfectly clear solution and were subsequently evaporated to dryness. Samples were then finally dissolved in a diluted nitric solution (~0.7 N) containing 10 ng/g of Sc, Ga, Mo, In, and Re used as internal standards for ICP-MS measurements.

Snow solutions (2–14 ml aliquots) were gently evaporated to dryness and then taken up twice in 7 N HNO_3 and subsequently evaporated. Solid residues were then taken up in the same ~0.7 N HNO_3 analysis solution containing internal standards.

Aliquots (0.5–1 g) of glassy material separated from the Hekla tephra (HK2000T) were leached at room temperature in 10 ml of either pure diluted HF solutions or diluted HF–HCl solutions with various F/Cl ratios (from 0.7 to 4.1). Experiments were conducted in Teflon containers at pH values between 2.4 and 3.1 for durations ranging between 10 min and 6 days. During soaking, the mixtures were regularly sonicated to enhance the interaction between the acid solution and the glassy material. At the end of the experiment, leaching samples were centrifuged and the supernatant solution was carefully pipetted. The glass fraction was rinsed twice with deionized water, centrifuged, and the supernatant solutions were added to the first one. These solutions were finally treated using the procedure described above for snow samples.

All trace elements were analyzed at the Laboratoire Magmas et Volcans in Clermont-Ferrand by ICP-MS (Fisons Plasma Quad II+) using external calibration. Duplicates of sample He27A were made to estimate reproducibility which is better than 5% for 70% of the analyzed elements and always better than 10% except for Zn (reproducibility of 15%) (see Appendix A). Accuracy of measurements was also checked by analyzing an international geological reference material provided by the USGS (Hawaiian Basalt BHVO-1). Values measured in Clermont–Ferrand for all trace elements are in close agreement with the ranges of recommended values (see Appendix A). Taken together, it suggests that 2σ uncertainties on our measurements usually are in the range 5–10% or better for most of the elements. Major element concentrations were measured by ICP-AES either in Clermont–Ferrand (HK2000L and HK2000T) or in SGAB Lulea (Sweden) (snow samples) with a 2σ uncertainty in the range 5–10%. Finally, volatile elements (SO_4^{2-}, Cl^-, and F^-) were measured by ionic chromatography at the Science Institute, University of Iceland in Reykjavik. Typical analytical uncertainties are of about 3% (2σ).

3. Results

Major element concentrations (given in wt.%) in samples HK2000L and HK2000T are given in Table 1. The 2000 eruption of Hekla produced a magma of intermediate composition, indistinguishable from those erupted in 1970, 1980, and 1991 (e.g., Baldridge et al., 1973; Gudmundsson et al., 1992; Sigmarsson et al., 1992).

Trace element concentrations in snow (expressed in ng g^{-1}) and lava (in μg g^{-1}) samples, along with typical blank values (in ng) obtained during chemical processing of samples, are given in Table 2. Both the lava flow and the tephra have similar trace element compositions. The chemistry blanks are largely negligible with only a few elements above detection limit of the ICP-MS instrument, for instance, Rb, Zr, Cd, Ba, La, Ce, Nd, and Pb having values $\geqslant$10 pg. The concentrations of these elements appear to be of the same order of magnitude as in the atmospheric background sample collected on Langjökull Glacier (L2). However, it is negligible compared to trace element contents in snow samples collected in the vicinity of Hekla.

Atmospheric precipitations in the highland of southern Iceland, as recorded by sample L2, have very low trace element concentrations. Most of the measured cations are at the picogram level or below the detection limit. Only a few elements, among which are the transition (Zn, Cu) and the alkali-earths metals (Sr, Ba), display significant concentrations (Table 2). Sr/Cl ratio and enrichments in Cu, Zn, Ba, and Sr observed in sample L2 reflect an actual enrichment of local precipitations due to marine aerosols as previously suggested by Gislason et al. (1996). Trace element contents in the atmospheric background remain most of the time negligible compared to those measured in snow samples of Hekla (from a factor of five up to six orders of

Table 1
Chemical composition of the most recent lavas produced at Hekla volcano

Samples	1970[a]	1980[a]	1991[a]	2000L	2000T
SiO_2	54.90	55.40	54.70	55.00	54.60
TiO_2	2.09	1.84	2.00	2.04	2.16
Al_2O_3	14.30	14.33	14.41	14.49	14.40
FeO	11.59	11.23	11.45	11.26	11.61
MnO	0.27	0.26	0.27	0.32	0.37
CaO	7.06	7.23	7.32	6.76	6.61
MgO	2.91	2.92	3.10	2.96	2.50
Na_2O	4.18	4.17	4.11	4.43	4.10
K_2O	1.22	1.30	1.23	1.23	1.23
P_2O_5	1.34	1.12	1.17	0.96	1.10
Sum	99.86	99.80	99.76	99.45	98.68

[a] From Gudmundsson et al. (1992).

Table 2
Analytical results of chemistry blanks, Hekla 2000 lava and tephra samples, and snow samples

Samples	Blank lava	HK2000L	HK2000T	Blank snow	L2	He14	He25	He27A	He27B	He28	He30
SiO_2	<ld	549,700	546,000	<ld	<64	396,000	16,000	169,000	169,000	176,000	13,500
Al	<ld	76,700	76,200	<ld	2.82	163,000	19,700	130,000	130,000	57,100	18,900
Be	0.210	3.17	3.11	<ld	<ld	12.8	1.35	11.7	11.6	13.5	1.65
Co	0.290	46.3	59.1	<ld	0.002	43.1	6.36	60.0	60.9	54.7	9.13
Cu	1.045	26.2	21.7	<ld	3.46	147	18.51	161	161	588	44.80
Zn	<ld	211	245	<ld	6.02	719	108	909	885	989	151
Rb	<ld	23.9	23.3	0.015	0.015	57.8	6.01	27.7	26.4	2.6	5.63
Sr	<ld	401	393	<ld	2.32	313	81.4	326	317	196	128
Y	0.010	73.9	72.0	0.002	<ld	191	8.12	18.2	15.6	1.87	1.43
Zr	0.455	465	502	0.016	0.007	1,375	217	1,252	1,217	1,362	203
Cd	<ld	0.186	0.634	0.137	<ld	91.4	11.0	98.6	97.8	120	19.9
Sb	0.085	0.144	0.127	0.004	<ld	0.732	0.083	0.617	0.600	0.456	0.026
Te	<ld	0.018	0.037	<ld	<ld	6.31	0.717	5.29	5.20	1.40	0.065
Ba	<ld	344	339	0.031	0.150	672	98.0	160	147	108	68.9
La	<ld	51.7	51.1	0.017	<ld	48.3	2.74	9.97	8.73	1.17	0.776
Ce	<ld	123	121	0.009	<ld	122	7.06	25.2	21.9	2.84	1.99
Pr	<ld	16.2	15.9	0.001	<ld	17.8	0.999	3.68	3.22	0.391	0.288
Nd	<ld	61.9	60.8	0.008	<ld	68.9	3.72	15.3	13.5	1.49	1.01
Sm	<ld	14.9	14.7	<ld	<ld	20.0	1.23	4.06	3.60	0.402	0.343
Eu	<ld	5.29	5.22	<ld	<ld	5.91	0.457	1.38	1.25	0.142	0.133
Gd	<ld	17.0	16.6	<ld	<ld	32.3	1.85	5.80	5.22	0.476	0.472
Tb	<ld	2.48	2.42	<ld	<ld	6.62	0.372	1.08	0.943	0.089	0.078
Dy	<ld	14.5	14.2	<ld	<ld	45.3	2.68	7.66	6.86	0.662	0.496
Ho	<ld	2.74	2.70	<ld	<ld	10.2	0.551	1.60	1.44	0.137	0.097
Er	<ld	7.56	7.47	<ld	<ld	29.8	1.66	4.61	4.20	0.444	0.275
Tm	<ld	1.00	0.985	0.001	<ld	4.18	0.236	0.655	0.597	0.069	0.035
Yb	<ld	6.08	5.99	<ld	<ld	25.4	1.49	4.18	3.76	0.454	0.241
Lu	<ld	0.906	0.895	<ld	<ld	3.93	0.217	0.587	0.530	0.070	0.035
Hf	0.040	11.1	10.9	<ld	<ld	22.7	5.05	30.2	30.1	30.4	3.30
Tl	0.025	0.080	0.141	0.002	<ld	18.3	1.96	11.2	10.6	13.7	1.71
Pb	<ld	3.25	3.30	0.074	<ld	57.2	5.95	21.1	15.7	23.1	0.520
Bi	0.050	0.024	0.038	<ld	<ld	0.820	0.044	0.253	0.139	0.024	<ld
Th	<ld	4.73	4.86	<ld	<ld	2.83	0.631	0.556	0.458	0.130	0.087
U	<ld	1.55	1.56	<ld	<ld	6.51	0.870	7.54	7.46	6.60	0.808
La/Yb	—	8.51	8.53	—	—	1.90	1.84	2.38	2.32	2.58	3.22
SO_4^{2-}	—	—	—	<ld	0.520	14.5	8	20	20	84	25
Cl^-	—	—	—	<ld	5.34	589	74	515	515	510	130
F^-	—	—	—	<ld	0.005	1257	107	832	832	448	85.9
F/Cl	—	—	—	—	<0.001	2.13	1.45	1.61	1.61	0.88	0.66
pH	—	—	—	—	—	2.55	3.5	3.1	3.1	3.51	4.46

Trace element concentrations are corrected from chemistry blanks and are given in nanogram per gram in snow samples, in nanogram in blanks, and in microgram per gram in both lava and tephra samples. SO_4^{2-}, Cl^-, and F^- in snow samples are given in microgram per gram. <ld, below detection limit, —, not determined. Note that detection limits for most of the elements range from less than 1 to 15 ppt except Be, Cu, and Zn whose detection limits are 20, 60, and 150 ppt, respectively.

magnitude higher). All analyzed trace elements, including not only volatile elements but also refractory elements such as REE and Th, are considerably enriched in snow samples collected near Hekla with respect to the atmospheric background. It suggests that the snow has been enriched when falling through the volcanic plume of Hekla. It is indeed well known that trace elements are considerably enriched in volcanic plumes as they form chemical compounds (mostly halides) that are gaseous at magmatic temperatures (e.g., Symonds et al., 1987, 1994). When the gas plume enters into the cold atmosphere, these volatile compounds are quenched to form solid particles (Withby, 1978) that are subsequently carried downwind in the diluted volcanic plume. In the case of a sub-Plinian to Plinian eruptive plume, the decrease in the plume temperature is slower than for passive degassing, which allows a time window for volcanic aerosols and gases to evolve chemically and physically (e.g., aerosol collision/aggregation processes, condensation of acid gases and magmatic water, and adsorption onto volcanic ash; see, for instance, Witham et al., 2005 and references therein). In such a regime, volcanic gases and aerosols, notably halogen species that have a much higher solubility than sulfur species, are also likely to be efficiently scavenged by magmatic water droplets (Textor et al., 2003). Even in the case of the 2000 Hekla eruption during which, regardless of snowstorms, magmatic water was quickly converted to ice in the volcanic plume (Rose et al., 2003), this scavenging effect of the halogen species is likely to have been efficient (Textor et al., 2003). It is thus likely that volcanic aerosols as well as

the most reactive gas species were quantitatively trapped by ice crystals within the eruptive plume and subsequently scavenged down to the ground by the snow that fell through the plume. On the other hand, it may be assumed in agreement with Textor et al. (2003) that only a small amount of the sulfur species (mainly SO_2 and H_2S) has been efficiently scavenged. It could notably explain the low-S content in our snow samples (see Table 2). Nonetheless, as far as trace elements are concerned, we may assume that the chemical composition of snow samples collected on the ground after the beginning of the eruption does represent that of the eruptive plume, keeping in mind that these samples represent an integrated path from the time of gas exsolution in the volcanic conduit to the time of sampling. This assumption was previously tested on Mt. Etna, where Le Guern (1988) showed that trace element concentrations and relative abundances in snow samples gathered at the summit during winter months were in excellent agreement with those measured in situ in gaseous emissions.

Trace element concentrations in snow samples of Hekla are not constant from one sample to another. For instance, samples He14, He27, and He28 appear to be the most concentrated while samples He25 and He30 are less enriched. This observation primarily relates to a different dilution of the plume in the atmosphere for each sample. However, data given in Table 2 show that the highest concentration recorded for a given trace element is not always observed in the same sample, suggesting that the chemical composition of snow samples does not depend on a dilution effect only. Major volatile species (SO_4^{2-}, F^-, and Cl^-) also present a similar behavior as illustrated by significant variations of their F/Cl ratios in the range 0.7–2.1. To assess the origin of trace element enrichments in snow samples, their volatility and mechanisms of transport in the volcanic plume of Hekla are characterized in the following section.

4. Trace element degassing at Hekla volcano

4.1. Trace element volatility

Intrinsic volatility of trace elements is often quantified through emanation coefficients ε (Pennisi et al., 1988; Rubin, 1997) or liquid–gas partition coefficients D (Gauthier et al., 2000). However, when it is impossible to determine the actual trace element concentrations in the pure gas phase because of its dilution in the atmosphere, volatility is most of the time determined on a relative scale through the use of an enrichment factor, EF. This parameter allows one to assess the volatility of any trace element compared to a reference element measured in both the gas phase and the solid phase (lava), according to the equation:

$$\mathrm{EF} = \frac{(X_\mathrm{G}/Y_\mathrm{G})}{(X_\mathrm{L}/Y_\mathrm{L})}, \qquad (1)$$

where X is the element of interest, Y is the reference element chosen for normalization, and subscripts G and L refer to gas (snow in the present study) and lava, respectively.

Aluminum has often been used as a normalizing element in EF calculations (e.g., Toutain et al., 2003) although Al has the major disadvantage to be a major element in magmas. Accordingly, the use of Al better describes the contribution of solid matter (spattered material, ash, or dust) to the gas phase rather than trace element volatility itself. It is thus recommended to use a volatile trace element at low-concentration levels in magmas to minimize this effect and, following Crowe et al. (1987), bromine is often chosen as the reference element for EF calculations. Nevertheless, any trace element fulfilling these two conditions (volatile enough to be significantly enriched in the gas phase, and at low concentrations in magmas to minimize ash contribution) would be suitable as a reference element, keeping in mind that EFs do not represent the absolute volatility of trace elements. In the lack of Br data, we use here Be as reference element due to its low content in Hekla lavas (Table 2) and because its abundance in snow samples primarily relates to the degassing of its chloride compounds (see discussion hereafter in Section 4.3).

Enrichment factors relative to Be, given in Table 3, show significant variations from one sample to another. For instance, $\mathrm{EF}_{(\mathrm{Th})}$ ranges between 0.01 and 0.31. REE display similar behavior, as well as some other trace elements well known to be volatile at magmatic temperatures (e.g., Bi with EFs in the range between 0.23 and 8.37). This variability confirms that trace element enrichments in these snow samples cannot be merely accounted for by variable dilutions of the volcanic plume. It may instead be related to variations in the chemical composition of the gas phase, notably in terms of F/Cl ratios (Table 2), following changes in the eruption dynamics and/or degassing mechanisms (e.g., Aiuppa et al., 2004).

Despite these variations, averaged enrichment factors can be calculated to represent the bulk volatility of trace elements at Hekla. They vary from 0.08 for the least volatile element (La) up to 150 for Cd, the most enriched element in snow samples of Hekla. Enrichment factors are plotted on an empirical scale of increasing volatility (Fig. 3). Based on breaks of slope (arbitrarily fixed at >30%) in Fig. 3, four classes of trace element volatility at Hekla may be distinguished. Refractory elements (group I) such as Th and LREE (from La to Sm) are characterized by EFs lower than 0.15. A second group of elements, composed of HREE (from Gd to Lu), Y, alkali-earths (Sr and Ba), Co, and Rb, is characterized by slightly increased EFs (between 0.15 and 0.50) although these elements remain poorly volatile. With enrichment factors higher than 0.5, other trace elements may be regarded as moderately (group III: $0.50 < \mathrm{EF} < 1.50$: Hf, Zr, Sb, Be, Zn, and U) to highly volatile (group IV: $\mathrm{EF} > 1.50$: Pb, Cu, Bi, Tl, Te, and Cd).

Table 3
Metal enrichment factors (EF) in the volcanic plume of Hekla

Samples	He14	He25	He27A	He27B	He28	He30	Mean (±SD)
Be	1.00	1.00	1.00	1.00	1.00	1.00	1.00 (0.00)
Co	0.23	0.32	0.35	0.36	0.28	0.38	0.32 (0.06)
Cu	1.35	1.35	1.62	1.64	5.23	3.02	2.37 (1.54)
Zn	0.84	1.14	1.16	1.14	1.10	1.32	1.11 (0.16)
Rb	0.60	0.59	0.31	0.30	0.26	0.45	0.42 (0.15)
Sr	0.19	0.46	0.22	0.21	0.11	0.60	0.30 (0.19)
Y	0.64	0.26	0.07	0.06	0.01	0.04	0.18 (0.24)
Zr	0.73	1.09	0.73	0.71	0.69	0.84	0.80 (0.15)
Cd	121	138	143	143	151	204	150 (28.3)
Sb	1.25	1.35	1.16	1.13	0.74	0.35	1.00 (0.38)
Te	86.2	92.3	79.1	78.5	18.2	4.9	59.9 (38.0)
Ba	0.48	0.67	0.13	0.12	0.07	0.38	0.31 (0.24)
La	0.23	0.12	0.05	0.05	0.01	0.03	0.08 (0.08)
Ce	0.25	0.13	0.06	0.05	0.01	0.03	0.09 (0.09)
Pr	0.27	0.14	0.06	0.05	0.01	0.03	0.10 (0.10)
Nd	0.27	0.14	0.07	0.06	0.01	0.03	0.10 (0.10)
Sm	0.33	0.19	0.07	0.07	0.01	0.04	0.12 (0.12)
Eu	0.28	0.20	0.07	0.06	0.01	0.05	0.11 (0.10)
Gd	0.47	0.25	0.09	0.08	0.01	0.05	0.16 (0.17)
Tb	0.66	0.35	0.12	0.10	0.01	0.06	0.22 (0.25)
Dy	0.77	0.43	0.14	0.13	0.01	0.06	0.26 (0.29)
Ho	0.91	0.47	0.16	0.14	0.01	0.07	0.29 (0.34)
Er	0.97	0.51	0.16	0.15	0.01	0.07	0.31 (0.37)
Tm	1.03	0.56	0.18	0.16	0.02	0.07	0.34 (0.39)
Yb	1.03	0.57	0.19	0.17	0.02	0.08	0.34 (0.39)
Lu	1.07	0.56	0.18	0.16	0.02	0.07	0.34 (0.40)
Hf	0.50	1.07	0.74	0.74	0.64	0.57	0.71 (0.20)
Tl	56.9	57.6	37.9	36.2	40.4	41.3	45.0 (9.60)
Pb	4.35	4.29	1.76	1.32	1.67	0.31	2.28 (1.66)
Bi	8.37	4.28	2.82	1.56	0.23	—	3.45 (3.13)
Th	0.15	0.31	0.03	0.03	0.01	0.04	0.09 (0.12)
U	1.04	1.31	1.31	1.31	1.00	1.00	1.16 (0.17)

EFs are calculated from Eq. (1) after the subtraction of the atmospheric background (sample L2).

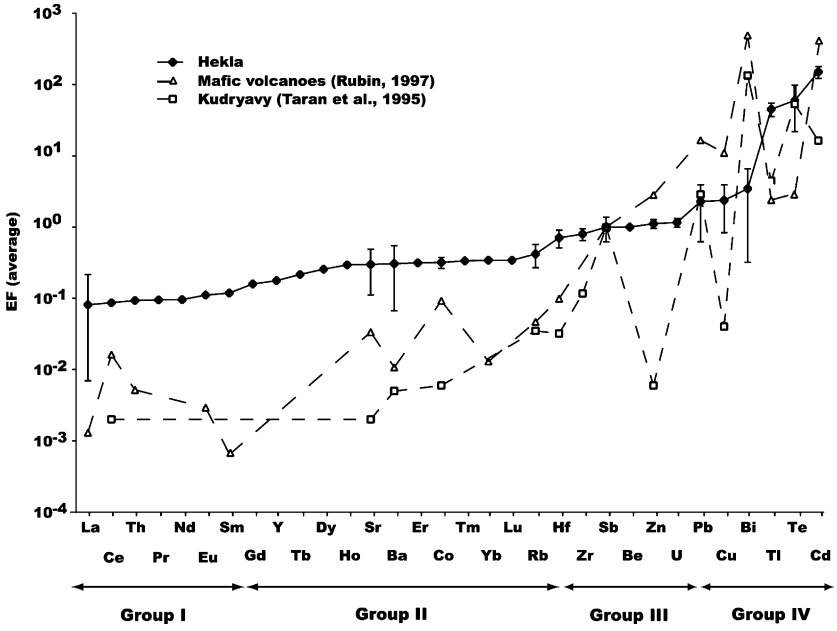

Fig. 3. Averaged enrichment factors for Hekla (this work), Kudryavy (Taran et al., 1995), and worldwide emissions from mafic volcanoes (Rubin, 1997) plotted on an empiric scale of increasing volatility. Standard deviations for Hekla data (Table 3) are plotted for all analyzed trace elements but Th and REE, which have similar error as La.

4.2. Comparison with other volcanoes

Not surprisingly, most of the trace elements from groups III and IV are all known to be volatile at magmatic temperatures and usually are considerably enriched in volcanic gases (e.g., Rubin, 1997; Gauthier and Le Cloarec, 1998). Regarding the first two groups, Th and REE usually are considered to be refractory elements that form non-volatile compounds (Gauthier and Le Cloarec, 1998; Aiuppa et al., 2003) while alkalis, alkali-earths, and cobalt usually are classified among moderately volatile trace elements (Hinkley et al., 1994; Rubin, 1997).

At first glance it thus seems that trace element volatilities at Hekla are similar to those previously observed on different active volcanoes worldwide. However, a more detailed comparison outlines some significant differences. Mean enrichment factors for trace elements in gases from mafic volcanoes (Rubin, 1997) are compared with those measured at Hekla (Fig. 3). Note that Rubin's (1997) database has been converted into EFs normalized to Sb as no data on Be are available in his study. It allows however direct comparison of the two datasets as antimony has the same volatility as beryllium at Hekla (Table 3). While the least volatile elements at Hekla (groups I and II) are also the least volatile ones in basaltic systems, they appear to be enriched by about one to two orders of magnitude at Hekla compared to the general trend. On the contrary, the most volatile elements at Hekla (groups III and IV) are also the most volatile ones at mafic volcanoes although most of them (but Hf, Tl, and Te) are less volatile in the present case. The same conclusions can be drawn when comparing data of Hekla with Sb-normalized EFs for high-temperature gases (825–940 °C) collected at Kudryavy (Kuril Islands), a dome-forming volcano which produces calk-alkaline basaltic andesites (Taran et al., 1995). EFs of Kudryavy are also reported in Fig. 3 and depict a similar trend. However, apart from Bi, volatilities at Kudryavy are of the same order or even lower than at Hekla, notably for Cu and Zn which are considerably depleted in gases of Kudryavy.

Trace element volatility in magmatic systems depends on the magma composition itself, the temperature of gas emission, and the occurrence of different volatile compounds in the gas phase (e.g., halides, sulfates, etc.). It is likely that the above-mentioned differences for the most volatile elements may be accounted for by variations in these parameters, trace element degassing being more efficient for basalts than for more differentiated magmas (e.g., Giggenbach, 1996). The enhanced volatility of REE and other refractory elements at Hekla is however difficult to explain in that way, unless they are preferentially degassed as volatile compounds that do not prevail at other volcanoes. Suitable candidates might be fluorides since gases of Hekla are characterized by high F/Cl ratios (between 0.7 and 2.1) while F/Cl ratios usually are much lower than 1 at most active volcanoes (Symonds et al., 1994). Such enrichments in fluorine have been already observed for previous eruptions of Hekla (e.g., Oskarsson, 1980, 1981; Sigvaldasson and Oskarsson, 1986) as well as for other Icelandic volcanoes (White and Hochella, 1992; Thordarson et al., 1996). High F/Cl ratios have also been observed in gases collected at other hot-spot related volcanoes including Kilauea (Gerlach, 1993) and Mauna Loa (Greenland, 1987) in Hawaii. They are likely related to a higher F content in deep hot-spot magmas compared to magmas from other geodynamical settings (Giggenbach, 1996 and references therein).

4.3. Trace element transportation in the volcanic plume of Hekla

Analyses of both volcanic gases and sublimates, as well as thermodynamic modeling (Gemmell, 1987; Symonds et al., 1987; Le Guern, 1988; Symonds et al., 1994), suggest that trace elements may be degassed and coexist under various forms in the gas phase. Among the most common compounds responsible for trace element degassing are halides (especially chlorides, but also fluorides and bromides), S-compounds (sulfates and sulfides), or even metallic species. If, as assumed here, no chemical fractionation of volcanic aerosols occurred during the plume scavenging by snow storms, volatile compounds should be preserved in snow samples. Because of the variable dilution of snow samples, one thus should expect linear correlations between the various cations and their bonding anions. This hypothesis has been tested for all trace elements from the four above-mentioned groups of volatility. Correlation coefficients (r) between either the three analyzed anions (SO_4^{2-}, F^-, and Cl^-) or the sum of halogens ($F^- + Cl^-$) and trace elements are given in Table 4 and some correlations are illustrated in Fig. 4. With the noticeable exception of bismuth and lead, all volatile trace elements (groups III and IV) display significant correlations either with sulfates (Cu; Fig. 4A), fluorides (Te; Fig. 4B), chlorides (Cd, Tl, U, Zn, Be (Fig. 4C), Zr, and Hf), or halogens (Sb). Among the least volatile trace elements (groups I and II), Co and Sr appear to be linked to chlorides while Rb is correlated with F^- in the plume of Hekla. On the other hand, none of the other refractory and poorly volatile elements present a significant linear relationship with any of the studied anions, even if their contents in snow samples increase with F concentrations (Fig. 4D).

As explained above, the linear correlations observed for some cations strongly suggest that their enrichment in the gaseous plume of Hekla is directly linked to a primary degassing process of their volatile compounds. Whenever available, boiling temperatures of these compounds (Lide, 1997) are reported in Table 4. It can be seen that for all advocated volatile compounds but RbF, $SrCl_2$, and $CoCl_2$, the boiling temperature is significantly lower than the magma temperature at Hekla, close to 1050 °C (Thorarinsson and Sigvaldasson, 1973), which confirms our hypothesis. In spite of the higher boiling temperatures of Rb, Sr, and Co compounds (1410, 1250, and 1049 °C, respectively; Ta-

Table 4
Correlation coefficients (r) between concentrations of trace elements and each of the analyzed anions (SO_4^{2-}, Cl^-, F^-, and $Cl^- + F^-$)

Samples	r (SO_4^{2-})	r (Cl^-)	r (F^-)	r ($Cl^- + F^-$)	Chloride	T_b (°C)	Fluoride	T_b (°C)	Other compounds	T_b (°C)
Group IV										
Cd	—	**0.946**	0.698	0.800	**$CdCl_2$**	960	CdF_2	1748		
Te	—	0.637	**0.959**	0.908	$TeCl_4$	387	**TeF_4**	195		
Tl	—	**0.927**	0.887	0.929	**TlCl**	720	TlF	826		
Bi	—	—	—	—	$BiCl_3$	447	BiF_3	900	**$BiBr_3$**	453
Cu	**0.928**	—	—	—	$CuCl_2$	630^{dec}	CuF_2	1676	**$CuSO_4$**	560^{dec}
Pb	—	—	0.827	0.747	$PbCl_2$	951	PbF_2	1293	**$PbBr_2$**	892
Group III										
U	—	**0.962**	0.818	0.889	**UCl_4**	791	UF_4	1417		
Zn	—	**0.929**	0.681	0.783	**$ZnCl_2$**	732	ZnF_2	1500		
Be	—	**0.981**	0.808	0.888	**$BeCl_2$**	482	BeF_2	1169		
Sb	—	0.948	0.956	**0.985**	**$SbCl_3$**	220	**SbF_3**	345		
Zr	—	**0.989**	0.833	0.901	**$ZrCl_4$**	331^{sp}	ZrF_4	912^{sp}		
Hf	—	**0.919**	0.697	0.790	**$HfCl_4$**	317^{sp}	HfF_4	970^{sp}		
Group II										
Rb	—	0.766	**0.941**	0.925	RbCl	1390	**RbF**	1410	**Rb**	688
Lu	—	—	—	—	$LuCl_3$	925^{T_m}	LuF_3	1182^{T_m}		
Yb	—	—	—	—	$YbCl_3$	875^{T_m}	YbF_3	1157^{T_m}		
Tm	—	—	—	—	$TmCl_3$	824^{T_m}	TmF_3	1158^{T_m}		
Co	—	**0.917**	0.714	0.801	**$CoCl_2$**	1049	CoF_2	1400		
Er	—	—	—	—	$ErCl_3$	776^{T_m}	ErF_3	1147^{T_m}		
Ba	—	—	0.663	—	$BaCl_2$	1560	BaF_2	2260		
Sr	—	**0.900**	0.876	0.912	**$SrCl_2$**	1250	SrF_2	2460		
Ho	—	—	—	—	$HoCl_3$	718^{T_m}	HoF_3	1143^{T_m}		
							HoF_3	2200		
Dy	—	—	—	—	$DyCl_3$	680^{T_m}	DyF_3	1154^{T_m}		
Tb	—	—	—	—	$TbCl_3$	588^{T_m}	TbF_3	nd		
Y	—	—	—	—	YCl_3	721^{T_m}	YF_3	1150^{T_m}		
Gd	—	—	—	—	$GdCl_3$	609^{T_m}	GdF_3	1231^{T_m}		
Group I										
Sm	—	—	—	—	$SmCl_3$	682^{T_m}	SmF_3	1306^{T_m}		
Eu	—	—	—	—	$EuCl_3$	623^{T_m}	EuF_3	1276^{T_m}		
Nd	—	—	—	—	$NdCl_3$	758^{T_m}	NdF_3	1377^{T_m}		
Pr	—	—	—	—	$PrCl_3$	786^{T_m}	PrF_3	1395^{T_m}		
Th	—	—	—	—	$ThCl_4$	921	ThF_4	1680		
Ce	—	—	—	—	$CeCl_3$	817^{T_m}	CeF_3	1430^{T_m}		
La	—	—	—	—	$LaCl_3$	859^{T_m}	LaF_3	1493^{T_m}		

Boiling temperatures (T_b) and/or melting temperatures (T_m) of the main halide compounds are reported (data from Lide, 1997). Based on the highest correlation coefficients (with $r \geqslant 0.900$), the most likely volatile compounds responsible for trace element transportation in volcanic gases are emphasized in bold characters. Note that no satisfactory regression is obtained for refractory elements (groups I and II), except for Co, Sr, and Rb.
—, linear regression lower than 0.6; nd, no data available; dec, decomposes; sp, sublimation point.

ble 4), their presence in the plume might also be related to primary degassing processes if they had a sufficient vapor pressure to be extracted from the molten magma into the gas phase, further explaining why these trace elements are only weakly volatile at Hekla. Alternatively, part of their enrichment might also be related to other processes as discussed later on in this paper.

While degassing of volatile halides (mainly chlorides) or sulfates appears to be the most likely explanation for most of the trace element enrichments in the volcanic plume of Hekla, it is surprising to observe that neither Pb nor Bi, two of the most volatile trace elements, correlates with any of the studied anions. In particular, $PbCl_2$ and $BiCl_3$ have low-boiling temperatures (Table 4) and are thought to be main carriers of Pb and Bi in volcanic gases (e.g., Le Guern, 1988). Nevertheless, Gemmell (1987) suggested that bromides may also act as efficient transporters of trace elements in volcanic gases. As both $PbBr_3$ and $BiBr_2$ have boiling temperatures lower than magma temperature at Hekla, they could be responsible for Pb and Bi enrichments in our samples. Unfortunately, no Br data are available in gases of Hekla and, thus, the validity of this hypothesis cannot be verified.

On the other hand, the observed enrichments in the most refractory elements (Th, Y, Ba, and REE) are difficult to reconcile with degassing processes alone as none of these elements correlate with the studied bonding anions. Furthermore, as shown in Table 4, their halide compounds (including bromides and iodides (data not shown); Lide, 1997) have high-melting temperatures (boiling temperatures are mostly unknown), which suggest that the magma temperature at Hekla is too low to ensure their volatilization. Accordingly, their abundance in the snow samples collected near Hekla calls for a different process than

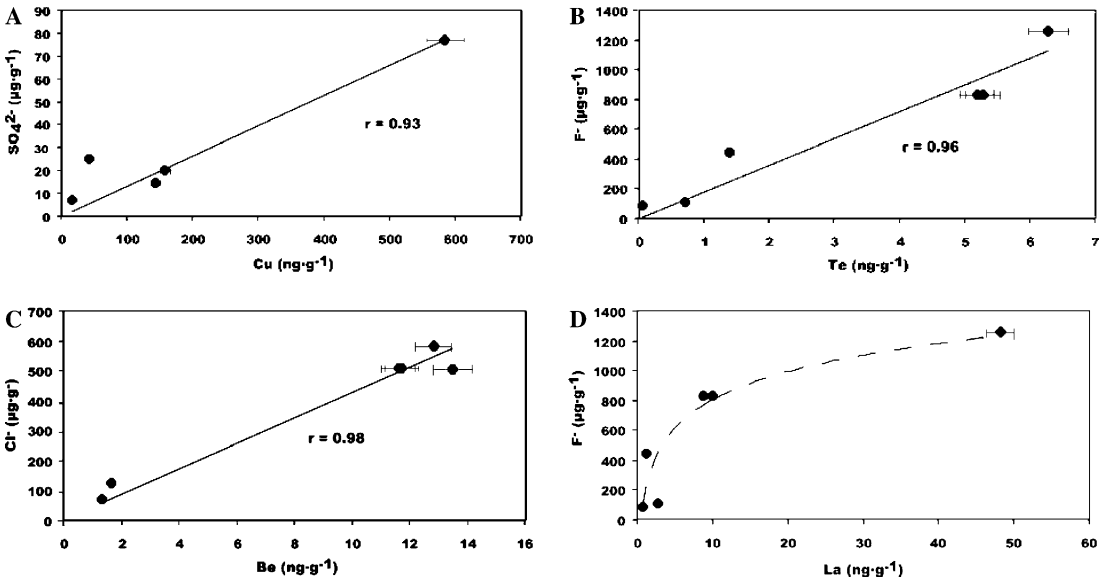

Fig. 4. Correlations between the studied volatile trace elements and their bonding anions. Note that refractory elements including Th and REE do not correlate linearly with any of the bonding anions. Error bars at 2σ are shown as well as regression coefficients r. (A) Linear correlation between Cu and SO_4^{2-}. (B) Linear correlation between Te and F^-, (C) Linear correlation between Be and Cl^-. (D) Relation between La and F^-.

primary magmatic degassing. To understand the observed enrichments in refractory elements, we will focus in the following sections on the specific behavior of REE.

5. Rare-earth enrichment at Hekla

5.1. Rare earth elements patterns in the volcanic plume of Hekla

The REE concentrations in snow samples are normalized to the 2000 lava flow composition and reveal strongly fractionated patterns as shown in Fig. 5. This fractionation is characterized by a significant enrichment of heavy rare earth elements (HREE) over light rare earth elements (LREE), with a (La/Yb)* ratio (defined as $(La/Yb)_{snow}/(La/Yb)_{lava}$) in the range 0.22–0.38. For most of the samples, the fractionation is observed for REE heavier than Eu, except for sample He30 where it starts at Sm.

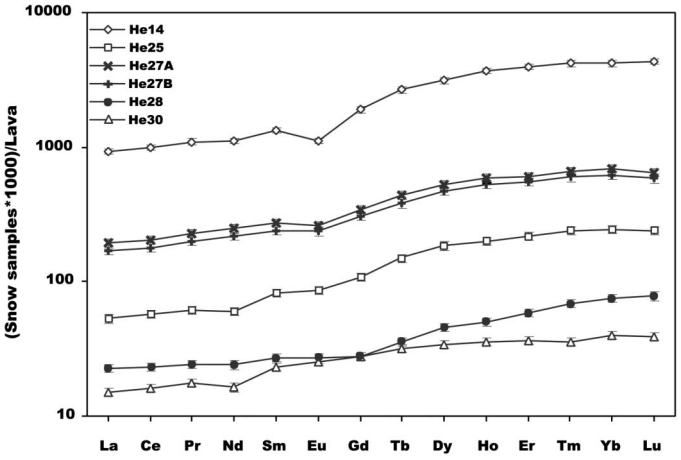

Fig. 5. REE patterns in snow samples normalized to the 2000 Hekla lava flow composition illustrating the fractionation of REE and the significant enrichment of HREE over LREE. Error bars are given at the 2σ confidence level.

To the best of our knowledge, no systematic study on REE mobility and fractionation in hot magmatic gases has been undertaken so far. Nevertheless, scarce data have been published elsewhere (e.g., Rubin, 1997 and references therein) underscoring their extremely low volatility. In fact, the occurrence of REE in gas samples is often considered as a marker of the presence of volcanic ash and dust in addition to the aerosol fraction (Gauthier and Le Cloarec, 1998; Aiuppa et al., 2003). Although the sub-Plinian plume of Hekla is obviously very enriched in tephra, this explanation cannot account for the observed REE enrichments since melted snow samples were filtered at 0.2 µm to get rid of all tephra. Although some very fine particles might have passed through the filters and could have been subsequently dissolved during the chemical treatment of samples, the REE fractionation observed at Hekla, contrary to what was observed on Etna (Aiuppa et al., 2003), eliminates this explanation.

Despite the lack of data about REE behavior in hot volcanic gases, these elements are known to be significantly mobile in natural hydrothermal systems (Michard and Albarède, 1986; Michard, 1989; Lewis et al., 1997). Compilations of experimentally determined reaction constants for REE-complexes at 25 °C and 1 bar (e.g., Wood, 1990a; Millero, 1992) show that REE complexation with ligands such as Cl^-, F^-, SO_4^{2-}, PO_4^{3-}, OH^- or CO_3^{2-} is potentially important in natural systems depending on the pH of the solution. In low-pH acidic solutions, the first four species usually prevail and the most concentrated anion acts as the most stable ligand. In volcanic-derived fluids, both

Cl^- and F^- usually are the dominant species so that REE are likely to be transported as chlorides and fluorides in such fluids (Haas et al., 1995). According to these authors, the stability of REE–chloride complexes increases relative to REE–fluoride complexes for low-F/Cl ratios under acidic conditions while REE–fluorides prevail over REE–chlorides for high-F/Cl ratios. Noteworthy, HREE are more strongly complexed by fluorides than LREE, whereas they are less strongly complexed by chlorides than LREE ($Kr_{F\text{-}HREE} > Kr_{F\text{-}LREE}$ and $Kr_{Cl\text{-}HREE} < Kr_{Cl\text{-}LREE}$ where K_r is the equilibrium constant of the complexation reaction; Haas et al., 1995; Wood, 1990a). This general behavior is enhanced at higher temperatures as REE complexation increases with temperature (Wood, 1990b) and REE-complex' stability, notably that of fluorides (Bilal and Langer, 1987; Luo and Millero, 2004), also increases with rising temperatures (Haas et al., 1995). On the other hand, a decrease in their stability is experimentally observed when pressure increases.

The acidic volcanic plume of Hekla is enriched in F over Cl and is characterized by much higher F/Cl ratios than usually observed at active volcanoes (Symonds et al., 1994). Accordingly, it should be expected that REE are mainly complexed and transported as fluorides in the volcanic plume. The observed fractionation and enrichment in HREE over LREE is also in good agreement with Haas et al.'s (1995) results, further suggesting that fluorides are indeed responsible for REE transportation in the volcanic plume of Hekla.

The question of how and when these fluorides may form must now be addressed. As shown earlier, it is quite unlikely that REE–fluorides are degassed at Hekla, based on both the too low magma temperature at Hekla that prevents the volatilization of such compounds, and the lack of linear correlation (dilution of volatile species in the atmosphere) between REE and F. Alternatively, the presence of REE–fluorides in the volcanic plume of Hekla may be caused by the vaporization of a shallow, F-rich hydrothermal system. It is however unlikely since there is no surface evidence of such a hydrothermal system at Hekla, which is thought to be linked to the young age of the volcano (Sigmarsson et al., 1992). Most likely, the observed REE enrichment and fractionation could be related to the interaction of a F-rich gas (or aerosol) phase with silicate rocks. This process may occur as soon as degassing initiates, that is within the magma conduit prior to the eruption of the sub-Plinian column. It may also occur within the eruptive plume itself where adsorption of volcanic gases and aerosols onto tephra is very fast and efficient (e.g., Witham et al., 2005), leading to favorable conditions for the dissolution of the silicate glass in contact with fluorine. Obviously the longer the exposure time of tephra in this F-rich environment is, the more efficient the dissolution is (e.g., Spadaro et al., 2002). Even if tephra became rapidly ice-coated during the 2000 Hekla eruption, it cannot be ruled out that dissolution went on (likely at a slower rate) once the eruptive plume was scavenged down to the ground by snowstorms, and even until snow solutions were prepared and filter at the laboratory.

To better understand how and when the hypothesized dissolution process occurred, we will use in the following section a theoretical approach based on thermodynamic considerations on silicate glass dissolution in a F-rich environment.

5.2. Tephra dissolution in the volcanic plume of Hekla: theoretical approach

As shown in Table 2, (La/Yb) ratios in snow samples vary from 1.84 to 3.22 while the same ratio is 8.51 in lavas from Hekla. This fractionation of REE in snow samples is obviously impossible to reconcile with a stoichiometric tephra grain dissolution. However, for a clarity purpose, it will be tentatively assumed that the observed REE enrichment and fractionation in snow samples of Hekla may be explained by the congruent dissolution of tephra grains. The stoichiometric dissolution rates ($\mathscr{D}$) of natural silicate glasses can be calculated taking into account both the compositions of glasses and aqueous solutions (Oelkers and Gislason, 2001; Gislason and Oelkers, 2003; Wolff-Boenisch et al., 2004a,b). Far-from-equilibrium glass dissolution rates ($\mathscr{D}$ in mol m^{-2} s^{-1}), normalized to geometric surface area, can be described by the following equation at 25 °C (Wolff-Boenisch et al., 2004a):

$$\log \mathscr{D} = (-0.086 \times [SiO_2] - 2.23) + (-0.0067 \times [SiO_2] + 0.683) \times \log(a^3_{H+}/a_{Al3+}), \quad (2)$$

where $[SiO_2]$ refers to the weight percent of SiO_2 in the tephra sample HK2000T (Table 1), and a_i denotes the activity of the aqueous species (H^+ and Al^{3+}) in snow solutions. This expression suggests that for a given silica glass composition and a constant total dissolved Al in the aqueous solution, dissolution rates depend on pH and ligands capable of complexing Al^{3+}, since aluminum exists as Al-complexes. At constant total dissolved Al and in the absence of other ligands than OH^-, dissolution rates decrease dramatically with increasing pH at acid conditions, minimize at near neutral conditions, and increase more slowly with increasing pH at basic conditions. Any ligand besides OH^- capable of complexing Al^{3+} will increase the dissolution rate, as it will decrease its activity ($a^{Al^{3+}}$, Eq. (2)). In the low-pH snow sample solutions, the main ligand capable of complexing Al^{3+} is most likely F^-. The aqueous activity of Al^{3+} can be calculated from the chemical composition of the five snow samples (Table 2) using the PHREEQC 2.6 computer code (Parkhurst and Appelo, 1999). With the glass composition, pH, and the $a^{Al^{3+}}$ given, the far-from-equilibrium dissolution rates, normalized to geometric surface area, are calculated according to Eq. (2). The results are reported in Table 5, and vary between 3.98×10^{-8} and 1.58×10^{-6} mol m^{-2} s^{-1}. The dissolution rates are the highest at low-pH and high-F concentration. These dissolution rates are up to four orders of magnitude higher

Table 5
Parameters and results of calculations for stoichiometric tephra dissolution

Samples	He14	He25	He27	He28	He30
d (km)	21	19.5	16	20	26
$m_{ice+snow}$ (g)	2387	2114	2241	1492	1557
m_{tephra} (g)	370	22	367	2197	717
$\phi > 5.6$ mm	52.0	0.00	0.00	35.7	40.7
$5.6 > \phi > 2.0$ mm	41.7	0.00	1.26	41.4	51.9
$2.0 > \phi > 1.0$ mm	5.10	0.00	6.35	14.9	4.11
$1.0 > \phi > 0.71$ mm	0.21	0.00	9.39	3.80	0.13
$0.71 > \phi > 0.50$ mm	0.05	0.00	17.3	1.47	0.05
$0.50 > \phi > 0.25$ mm	0.06	0.00	28.5	0.54	0.13
$\phi < 0.25$ mm	0.95	100	37.1	2.06	2.93
A (m^2)	0.25	0.34	2.94	2.45	0.71
$\mathscr{D}$ (mol m^{-2} s^{-1})	1.58×10^{-6}	3.16×10^{-7}	1.26×10^{-6}	7.94×10^{-7}	3.98×10^{-8}
Q_v (mg)	50	10	442	232	3
La theoretical (ng g^{-1})	1.01	0.31	10.07	7.93	0.11
La measured (ng g^{-1})	48.3	2.74	9.97	1.17	0.78
Leaching contribution (%)	2.1	11.2	108	678	14.1
Yb theoretical (ng g^{-1})	0.12	0.04	1.18	0.93	0.01
Yb measured (ng g^{-1})	25.4	1.49	4.18	0.45	0.24
Leaching contribution (%)	0.47	2.41	29.7	207	5.36

d is the distance to the vent of each sampling site. $m_{ice+snow}$ refers to the total mass of aqueous solution while m_{tephra} represents the total mass of dried (water-free) tephra contained in snow samples. ϕ (in %) is the grain size distribution among the different granulometric fractions given in millimeter. A is the total available tephra exposure surface in collected snow samples. $\mathscr{D}$ are calculated dissolution rates and Q_v represents the quantity of dissolved glass assuming stoichiometric dissolution (see text for explanation).

than those reported by Oelkers and Gislason (2001) and Wolff-Boenisch et al. (2004b) for natural silicate glass dissolution in the absence of fluoride. On the other hand, $\mathscr{D}$ values obtained by Wolff-Boenisch et al. (2004a) in high-F content dissolution experiments match those calculated for the least-concentrated snow solutions of Hekla (He25 and He30). The quantity of dissolved glass in the aqueous solution during melting assuming stoichiometric dissolution (Q_v in g) can be calculated by the following equation:

$$Q_v = D \times A \times t \times M_v, \quad (3)$$

where A is the total geometric surface area of the glass in contact with water (in m^2), t is the duration of dissolution process (in s), and M_v is the molar mass of the glass determined from the chemical composition of HK2000T (66.20 g mol^{-1}). The efficiency of the dissolution process and hence the amount of elemental leaching from the tephra grains increase with both time and the available exposure surface of tephra grains.

The duration of the interaction between the F-rich gas phase of Hekla and the solid material is difficult to constrain precisely. It obviously depends on where and when the dissolution process initiated, that is either within the volcanic conduit, within the eruptive plume, or even in the laboratory during sample preparation. The duration of the dissolution process thus remains mostly unknown except for the latter case (30 min of melting at 0–25 °C). The potential stoichiometric release of major and trace elements in the laboratory during sample preparation can thus be calculated according to Eq. (3) using the chemical composition of the Hekla 2000 tephra (Table 1). The tephra geometric surface area A was calculated for each sample from its grain size distribution assuming that tephra grains have a spherical shape and a density of 2610 kg m^{-3} for a basaltic andesite (Table 5). This estimate neglects surface heterogeneities, notably open pores that may increase the specific surface area (A_s) available for dissolution by about one order of magnitude in the case of Hekla tephra (Delmelle et al., 2005).

Knowing both $\mathscr{D}$ and A, the total mass of leached material Q_v is calculated from Eq. (3) (Table 5). This calculation assumes that all the geometric surface of the glass, A, is in active contact with all the melt water for the whole melting period, 30 min. This condition was obviously not met for sample He28, which contains a large excess of tephra compared to the amount of liquid as reflected by its high glass to snow mass ratio (Table 5). The estimates obtained for both La and Yb (Table 5) are compared with measured concentrations in snow samples. The calculated contribution of the leaching process during snow melting exceeds by far the measured concentrations in the sample He28 due to the above-mentioned reasons. However, in all other samples, the REE enrichment gained by the congruent dissolution of tephra grains during sample preparation is significantly lower than the actual concentrations measured in the snow solutions, for both Yb and to a lesser extent La. Even if we consider the specific surface area (A_s) available for dissolution instead of a simple geometric surface (A), increasing the amount of leached REE by one order of magnitude would not be enough to account for the observed Yb enrichments in samples He14, He25, and He30. Furthermore, the REE contribution gained during the preparation of snow solutions at the laboratory is likely lower than that given in Table 5. Tephra dissolution in the

F-rich water indeed occurred at temperatures slightly above 0 °C for most of the melting duration, while dissolution rates $\mathscr{D}$ are calculated for 25 °C. Although a part of the REE enrichment observed in our samples was acquired during sample preparation, it is likely that tephra dissolution started as soon as the eruptive plume was emitted at the summit vent of Hekla, or even before its emission, that is within the magma conduit.

5.3. Tephra dissolution in the volcanic plume of Hekla: experimental approach

To further constrain the contribution of tephra grain dissolution in a F-rich environment to the chemistry of snow samples, leaching experiments were performed in the laboratory on fresh Hekla tephra. Experimental protocols as well as analytical procedures were detailed in Section 2.2 and used parameters are given in Table 6 along with analytical results.

REE patterns normalized to the 2000 tephra composition obtained during the leaching experiments are shown in Figs. 6A–D. As expected for partial dissolution of tephra grains in a F-rich environment, all experiments produced a significant fractionation of REE, marked by an enrichment of HREE over LREE. Nevertheless, the REE fractionation appears to be slightly less pronounced than in natural snow samples (Fig. 6A). This is underscored by the (La/Yb)* ratios of the experiments that range from 0.62 to 0.78 while those of the snow samples span the range 0.22–0.38. It can be seen in Fig. 6A that LREE (from La to Dy) patterns of the experiments match quite well those of the natural snow samples as they both display a significant increase in normalized REE contents, starting from Sm and/or Eu. On the other hand, experimental patterns show a progressive depletion of REE contents from Dy to Lu, which is not observed in natural snow samples. HREE experimental patterns appear to be somewhat intermediate between those recorded in snow samples (which are thought to be produced by the non-stoichiometric dissolution of magma or tephra) and flat patterns that would be obtained for a complete congruent dissolution process. Accordingly, experimental patterns may be explained by a near-stoichiometric dissolution process, which means that natural conditions prevailing at Hekla could not be exactly reproduced at the laboratory. Nonetheless, this experimental study of tephra dissolution in F-rich aqueous solutions may be used to estimate the role of some parameters on tephra dissolution processes in a F-rich environment.

Table 6
Experimental conditions for leaching experiments and chemical compositions of resulting aqueous solutions

Samples	Experiment A	Experiment B	Experiment C	Experiment D	Experiment E	Experiment F	Experiment G	Experiment H	Experiment I
Grain size	0.16–0.25	0.10–0.16	0.10–0.16	0.10–0.16	0.10–0.16	0.10–016	0.10–016	0. 10–016	0.10–016
$[HF]_{solution}$	31.6	31.6	27.12	80.4	80.4	80.08	153.1	80.08	80.08
$(F/Cl)_{solution}$	—	—	0.72	2.14	2.14	2.13	4.08	2.13	2.13
pH	3.11	3.11	2.80	2.60	2.60	2.45	2.35	2.45	2.45
m_{tephra}	0.96	0.98	1.00	1.01	0.50	1.01	0.99	1.00	0.91
Time	1440	1440	50	50	50	10	10	30	8640
F/tephra	0.32	0.31	0.25	0.80	1.60	0.73	1.50	0.76	0.83
La	22.0	23.0	49.7	67.2	81.7	65.4	88.0	63.0	101
Ce	49.2	53.9	117	167	201	172	239	164	254
Pr	6.35	7.09	16.2	23.6	28.2	23.9	33.8	22.8	33.7
Nd	23.6	26.5	57.8	86.1	103	88.3	124	84.0	123
Sm	6.67	7.32	16.1	23.2	28.8	26.0	36.4	24.3	34.5
Eu	2.61	2.81	5.63	8.64	9.81	9.43	13.2	8.70	12.3
Gd	9.60	10.2	21.4	32.8	37.1	32.5	45.0	29.5	43.5
Tb	1.41	1.50	3.21	4.98	5.58	4.81	6.91	4.53	6.37
Dy	8.80	9.33	19.7	30.3	33.7	29.8	43.1	27.68	38.1
Ho	1.61	1.68	3.59	5.44	6.22	5.33	7.66	5.01	6.94
Er	4.41	4.55	9.67	14.8	16.8	14.5	20.6	13.5	19.0
Tm	0.61	0.63	1.25	1.87	2.21	1.83	2.65	1.74	2.50
Yb	3.73	3.83	7.57	11.6	13.3	11.4	16.6	10.9	15.3
Lu	0.54	0.54	1.08	1.60	1.91	1.57	2.26	1.52	2.17
La/Yb	5.89	6.00	6.56	5.78	6.12	5.76	5.30	5.78	6.63
Co	28.1	26.6	26.2	49.3	55.7	59.2	127	64.8	83.5
Rb	20.3	19.0	22.3	29.0	31.8	36.7	59.9	38.8	39.2
Sr	733	755	761	947	907	1132	1583	1131	1342
Y	42.4	39.2	76.6	101	116	93.3	129	92.8	151
Ba	325	282	514	643	696	1230	1167	763	752
Th	2.02	1.98	3.62	4.22	5.64	6.55	8.85	5.87	5.13

Tephra grain size is given in millimeter. [HF] refers to the HF concentration (in $\mu g\ g^{-1}$) in the starting solutions. m_{tephra} refers to the weight of tephra (in g) initially contained in 10 ml of aqueous solution. The duration of the experiments is expressed in minutes. F/tephra mass ratio is expressed in $mg\ g^{-1}$. Note that analytical results (given in $ng\ g^{-1}$) have been recalculated for all experiments, but Experiment E, to 1 g of tephra to make easier the comparison between the different leaching experiments.

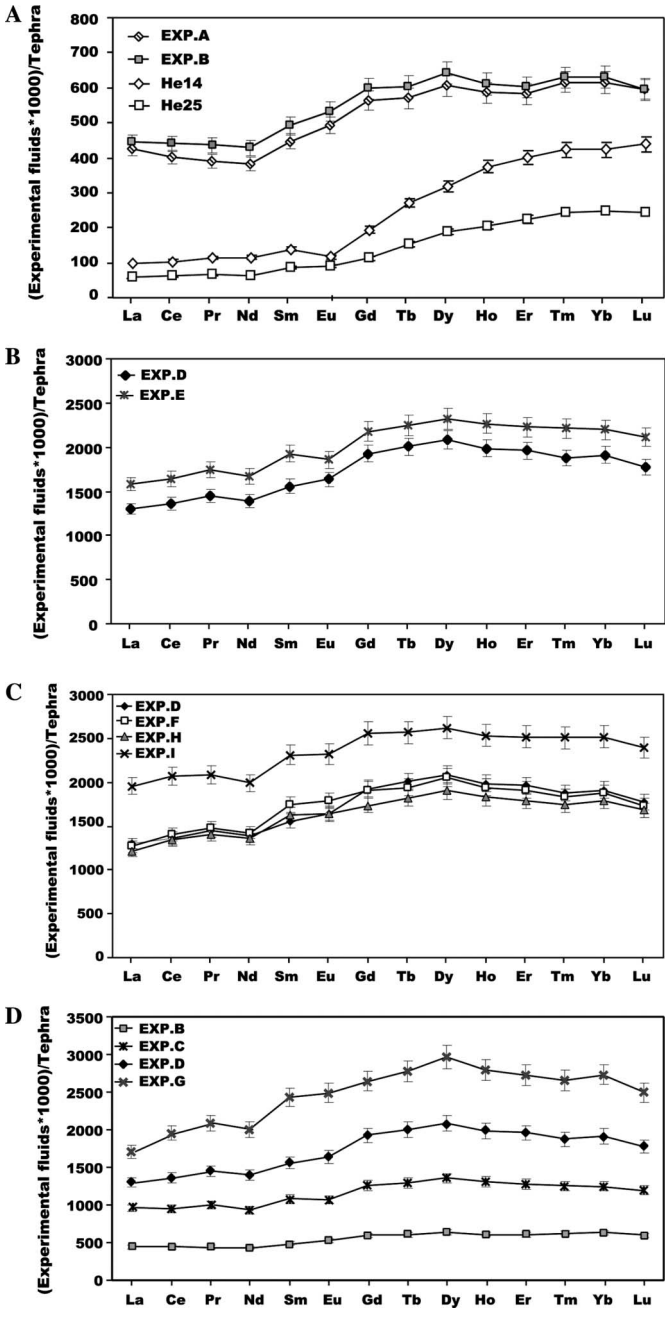

Fig. 6. REE patterns obtained during leaching experiments normalized to the 2000 tephra composition. Error bars are given at the 2σ confidence level. To constrain the effects of the different parameters on tephra dissolution processes, REE patterns are shown for different variables: (A) grain sizes of the starting material (in the range of 0.16–0.25 mm for Experiment A, and 0.10–0.16 mm for Experiment B). REE patterns of samples He14 (scaled down by a factor of 10 for a clarity purpose) and He25 are also shown for direct comparison between natural and experimental patterns. (B) Aqueous solution-to-tephra mass ratios; the amount of starting material soaked in 10 ml of aqueous solution is 1 g in Experiment D and 0.5 g in Experiment E. (C) Durations of dissolution experiments; Experiments D, F, H, and I ran for 50, 10, 30, and 8640 min, respectively. (D) F/Cl mass ratios; Experiments C, D, and G were performed with a F/Cl ratio of 0.7, 2.1, and 4.1, respectively, while Experiment B was carried out with a pure hydrofluoric solution.

5.3.1. Grain size distribution of the starting material

Experiments A and B were performed under the same conditions, except for the grain size distribution of the starting material which was in the range 0.16–0.25 and 0.10–0.16 mm, respectively. Both experiments produced very close REE patterns displaying a similar REE fractionation characterized by (La/Yb)* ratios of 0.69 and 0.70, respectively (Fig. 6A). Nevertheless, taking into account the overall analytical uncertainty, it appears that REE are slightly, but significantly, more enriched in Experiment B than in Experiment A. This shows that the finer the material is, the more efficient the dissolution is, which underscores the role played by the total exposure surface of the tephra grains as discussed in Section 5.2.

5.3.2. Aqueous solution-to-tephra mass ratio

Experiments D and E were carried out with the same parameters, only varying the amount of starting materials (1 and 0.5 g of tephra in Experiment D and Experiment E, respectively). It can be seen in Fig. 6B that the dissolution is much more efficient for Experiment E that has a higher aqueous solution to tephra mass ratio. On the other hand, the HREE/LREE fractionation is indistinguishable in these two experiments with (La/Yb)* ratios of 0.68 (Experiment D) and 0.72 (Experiment E). This set of experiments suggests that REE release is much more important when, at constant fluoride content in aqueous solution, a small amount of material is dissolved to a greater extent than a large quantity of material is dissolved to a small extent. This behavior could thus explain why the theoretical estimate of the leaching contribution during snow sample He28 melting (see Section 5.2) produced such largely overestimated results, most likely due to its tephra to snow ratio being larger than one.

5.3.3. Duration of the dissolution process

Four experiments were carried out (D, F, H, and I; Table 6) with time as the only variable, to check the time-dependency of dissolution efficiency. The resulting REE patterns are shown in Fig. 6C. Experiments ran for 10, 30, and 50 min (F, H, and D, respectively) exhibit very similar REE patterns characterized by a constant (La/Yb)* ratio of 0.68. It thus appears that on short timescales, the duration of the dissolution process is unable to produce significant differences in the amount of REE released from the tephra grains. On the other hand, the long-lasting experiment I (6 days) leads to a much higher REE release characterized by a higher (La/Yb)* ratio of 0.78. It suggests that the dissolution process at ambient temperature tends to reach a stoichiometric state after several days, or even hours, in agreement with Oelkers and Gislason (2001).

5.3.4. F/Cl mass ratio

Finally, another set of experiments was carried out to estimate the influence of the F/Cl ratio of the aqueous solution on the dissolution of tephra grains. All experiments having a F/Cl ratio in the range 0.7–4.1 (Experiments C,

D, and G) were run for short durations (10–50 min) while another experiment carried out with a pure hydrofluoric solution was conducted over a whole day (Experiment B). It can be immediately seen in Fig. 6D that the Experiment B gave rise to a significantly lower REE release than the other ones, in spite of a longer duration. It means that even if fluorides are mostly responsible for silicate dissolution, the dissolution efficiency is enhanced in the presence of chlorides. On the other hand, in the presence of both fluorides and chlorides, tephra dissolution becomes more and more important for increasing F/Cl, that is for increasing F contents at constant pH values. Interestingly, the most enriched REE patterns are also the most fractionated ones with (La/Yb)* ratios varying from 0.77 to 0.62 for a F/Cl ratio ranging between 0.7 and 4.1, respectively. This behavior is the reverse of what was observed for the effect of duration for which the most enriched REE patterns were characterized by higher (La/Yb)* ratios. It underscores the major role played by the F/Cl ratio of the aqueous solution on both the efficiency of silicate dissolution and the magnitude of REE fractionation, in agreement with Haas et al.'s (1995) results on REE complexation in acidic solutions.

5.4. Implications for REE enrichment and fractionation in the volcanic plume of Hekla

Clearly, REE patterns observed in snow samples from Hekla are most likely explained by the dissolution of silicate glass by a F-rich gas phase. This process was initiated either in the magma conduit or within the eruptive plume and likely went on until the filtration of snow solutions at the laboratory. At this point however, it remains unclear why natural REE patterns found in snow samples differ from those obtained during leaching experiments at the laboratory. As previously stated, the former might correspond to a very immature, non-stoichiometric dissolution process while the latter were produced during closer-to-stoichiometry experiments. According to both theoretical considerations and dissolution experiments described above, the kinetics of the dissolution process to reach its congruent state should depend on several parameters: the F/Cl mass ratio of the gas phase, the amount of solid material to be dissolved with respect to its gas content (especially its F content), the duration of the dissolution process, and the available exposure surface of solid particles.

In the dissolution experiments, the used range of F/Cl mass ratios (between 0.7 and 4.1) thoroughly overlaps the range of these ratios in natural snow samples (0.7–2.1), eliminating this parameter from being responsible for the differences between experimental and natural REE patterns.

Dissolution experiments performed at the laboratory contained between 0.3 and 1.6 mgF/g of tephra, while measured F/tephra mass ratios at the different sampling sites vary from 0.2 up to about 10 mgF/g of tephra (see Tables 2, 5, and 6). In agreement with both theoretical considerations (e.g., Wolff-Boenisch et al., 2004a) and experimental results, higher F/tephra mass ratios lead to a more efficient dissolution process. However, it is worth noting that Experiment C was carried out using parameters similar to those recorded for samples He28 and He30 but produced a (La/Yb)* ratio of 0.77 instead of 0.30 and 0.38 for He28 and He30, respectively. Accordingly, differences in the F/tephra mass ratio cannot account for the discrepancy between natural and experimental REE patterns.

As explained in Section 5.2, the duration of the dissolution process leading to the observed REE enrichment and fractionation is difficult to constrain precisely. According to geophysical measurements emphasizing the triggering of the eruption (Lacasse et al., 2004), dissolution may have lasted a few hours if the process initiated prior to the emission of the sub-Plinian column. Considering the average plume velocity (Lacasse et al., 2004) and the distance to the vent from each sampling site (Table 5), it may have lasted only 10–15 min if it occurred within the eruptive plume itself, or even less than that if dissolution was efficient only during the earliest stage of the eruption, that is before tephra become ice-coated. The contribution of each stage as well as the potential enrichment gained during sample preparation cannot be easily deconvolved. Nonetheless, since longer durations for tephra interaction with a F-rich fluid lead to a more mature and closer-to-stoichiometry dissolution process, natural REE patterns could be achieved only for gas–tephra interactions much shorter than 10 min. It would thus imply that tephra dissolution at Hekla occurred very rapidly, constraining the dissolution process to take place within the ascending sub-Plinian column at the moment of volatile adsorption onto solid particles.

The discussion of the influence of the available exposure surface of tephra grains is much more complex. First, while dissolution processes are slightly enhanced for smaller grain size fractions (Experiment B vs. Experiment A) in agreement with the theory (e.g., Wolff-Boenisch et al., 2004a,b), those experiments performed on a rather restricted range of grain sizes do not show significant variations of the (La/Yb)* ratio of the aqueous solution. It is thus difficult to fully appreciate the effect of this parameter on the magnitude of the fractionation. Second, experiments were carried out using a limited range of grain sizes (from 0.10 to 0.25 mm) while the actual grain size distribution of tephra within the eruptive plume of Hekla is much more variable and contains both finer and coarser fractions. Finally, wherever the dissolution process initiated, that is within the magma conduit versus within the eruptive plume, the total exposure surface of magma and/or tephra grains, available for the dissolution process likely varied through time. It is indeed obvious that the exposure surface in the magma conduit was much lower before than after magma fragmentation. Once the sub-Plinian plume was erupted, the total exposure surface also slightly decreased following the sedimentation of the denser and/or larger solid particles. In the lack of any further experimental constraints, REE budgets and fractionation in natural snow

samples could thus be tentatively linked to the variability of the total exposure surface of tephra grains. Nevertheless, it is reasonable to assume that REE budgets are likely governed by the partial dissolution of the finest (<100 μm) particles that offer the highest specific surface area for efficient dissolution by F-rich gases and aerosols. It implies again that most of the REE enrichment and fractionation is likely gained within the eruptive plume where volatile adsorption onto tephra is the most efficient (e.g., Witham et al., 2005).

In addition to the four parameters discussed above, temperature is still another parameter that may govern the kinetics of the reaction and hence its stoichiometric state. While experiments were carried out at room temperature (~25 °C), temperature in the magma conduit was obviously much higher (~1050 °C), and atmospheric temperatures estimated at the altitude of the volcanic plume (between 9 and 12 km) were much lower, around −60 °C (Lacasse et al., 2004). Adsorption of HF onto ash is temperature dependent and occurs at temperature below 600 °C (Oskarsson, 1980), suggesting that the process initiated after the emission of the sub-Plinian column. Moreover, since the dissolution process is inhibited at lower temperatures and enhanced at higher temperatures (Gislason and Oelkers, 2003), the non-congruent dissolution process at Hekla could be accounted for by making the assumption that dissolution occurred at low temperature. Taking all these considerations together (notably short duration, high available exposure surface, and low temperature), it thus seems that REE patterns recorded in snow samples of Hekla are most likely due to dissolution of tephra within the eruptive plume, even if a small contribution from the sample preparation process at the laboratory cannot be ruled out.

Beside the discrepancy between experimental and natural REE patterns, it is now interesting to address the question of the variability of REE enrichments and fractionations among the different snow samples. As expected from the theory of silicate dissolution in F-rich aqueous fluids (Eq. (2); Wolff-Boenisch et al., 2004a), dissolution efficiency depends, at a given F/Cl mass ratio, on temperature, duration, exposure surface of tephra grains, and fluorine content with respect to the amount of solid material to be dissolved. Since atmospheric temperatures remained constant throughout the first days of the eruption (Lacasse et al., 2004) and since the effects of dissolution duration for short-scale variations are negligible, REE release should be only governed by the F to exposure surface ratio (expressed in mgF/m^2) of each sample. As already pointed out, the total exposure surface interacting with fluorine is difficult to exactly quantify due to the sedimentation of some particles between the eruptive vent and the different sampling sites. However, we can tentatively make the assumption that it is proportional to the total amount of solid material preserved in each snow sample. A linear relationship between the logarithm of (La/Yb)* and the F/tephra mass ratios is actually observed for snow samples of Hekla (Fig. 7). It thus appears that the magnitude of REE fractionation mostly depends on the amount of fluorine available for tephra dissolution, as predicted by theory. On the other hand, such a correlation does not exist between log(La)* and the F/tephra mass ratio. REE release during dissolution processes is thus not entirely controlled by the fluorine content in the aqueous fluid. In agreement with Haas et al. (1995) and dissolution experiments discussed above, the dissolution reaction should actually be enhanced in the presence of chlorine. Such a behavior is confirmed for snow samples of Hekla since REE enrichments characterized by log(La*) are indeed correlated with the (F × Cl)/tephra mass ratio (Fig. 8).

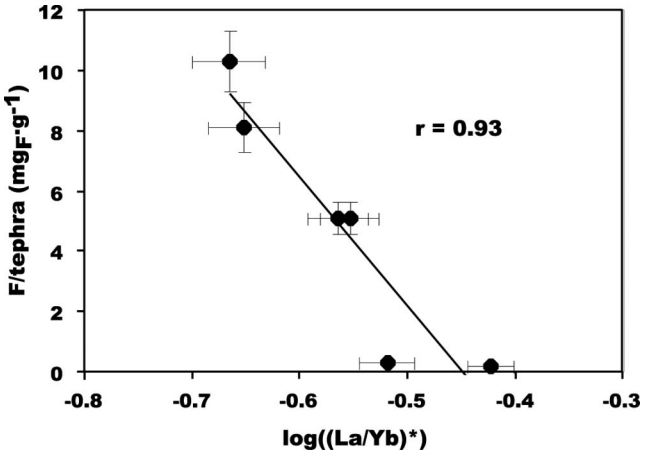

Fig. 7. Linear correlation observed between the magnitude of REE fractionation characterized by log((La/Yb)*), where (La/Yb)* is the lava-normalized (La/Yb) ratio of snow samples, and F/tephra mass ratio in snow samples suggesting the dependence of REE fractionation on the amount of fluorine available for tephra dissolution. Error bars are given at the 2σ confidence level.

It is obvious that the dissolution process governing REE distribution in snow samples of Hekla also plays a role in the abundance of other trace elements. This is especially true for other refractory elements that do

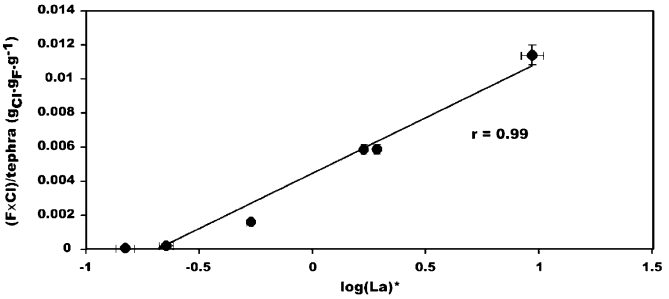

Fig. 8. Linear correlation observed between REE enrichments characterized by log(La)*, where (La)* is the lava-normalized La concentration in snow samples and (F × Cl)/tephra mass ratio in snow samples, suggesting that tephra dissolution and subsequent REE enrichment in the aqueous phase are enhanced in the presence of chlorine. Error bars are given at the 2σ confidence level.

not correlate with any bonding anions (e.g., Th, Y, and Ba). Experimental results presented in Table 6 confirm that leaching processes do mobilize significant amount of these trace elements. The same holds true for other weakly volatile trace elements such as Sr, Co, and Rb from the second group of volatility (see Fig. 3). Their abundance in the volcanic plume of Hekla is thus likely governed by both the magmatic degassing and the tephra dissolution processes. As laboratory experiments were realized near stoichiometric conditions while actual dissolution within the plume of Hekla is much further from stoichiometry, it is however impossible to exactly quantify the respective contribution of each process. Although the behavior of moderately to highly volatile elements (groups III and IV in Fig. 3) during dissolution processes was beyond the scope of this paper, it is worth mentioning that some of them (provided they are significantly abundant in magmas and readily mobile in F-rich fluids (e.g., Zr)) might also be enriched in the aqueous fraction of gaseous plume due to tephra–gas interactions.

6. Conclusion

Taking advantage of the heavy snow showers that condensed and scavenged down to the ground the eruptive plume of Hekla volcano during its last eruption in February 2000, the chemical composition of the gaseous phase released during a sub-Plinian eruption has been estimated for the first time. Trace elements (including alkalis, alkali-earths, transition metals, metalloids, heavy metals, actinides, and lanthanides) as well as sulfates, chlorides, and fluorides were analyzed in snow samples collected in the vicinity of Hekla shortly after the beginning of the eruption. All analyzed trace elements and anions are considerably enriched in the eruptive plume of Hekla compared to the standard atmospheric composition in southern Iceland. Trace element volatility at Hekla has been appraised through the use of enrichment factors relative to beryllium. As usually observed on other active volcanoes, trace elements that form volatile compounds at magmatic temperatures (e.g., transition metals, heavy metals, and metalloids) are the most enriched in the eruptive plume of Hekla. However, their volatility is lower than that at mafic volcanoes, which is thought to reflect both the lower temperature and higher degree of magma differentiation at Hekla. Volatile trace element contents in snow samples show positive linear correlations with one or several of the analyzed anions, suggesting that these trace elements are degassed at depth during primary degassing processes and are transported in the gas phase as chlorides, fluorides, and/or sulfates. More surprisingly, known refractory elements such as Th, Y, Ba, and lanthanides (REE) are also considerably enriched in the eruptive plume of Hekla. A strong fractionation of REE is further observed, HREE being considerably enriched over LREE. Such patterns are best explained by the presence of REE–fluoride complexes in the eruptive plume of Hekla. The too high-boiling temperature of such compounds and the lack of correlation between REE and F^- and/or the other analyzed anions suggest that REE enrichments at Hekla are not due to degassing processes. Both thermodynamic considerations and experiments carried out at the laboratory to constrain REE mobility during tephra dissolution in F-rich aqueous fluids show that partial dissolution of silicate glass may release significant amounts of REE characterized by such an enrichment in HREE over LREE. Taken together, the REE enrichments at Hekla are best explained by non-stoichiometric dissolution of tephra in a F-rich gas phase. The efficiency of dissolution and the subsequent enrichment in REE are mostly controlled by the amount of fluorine in contact with tephra, but are also enhanced in the presence of chlorine. On the other hand, the magnitude of the fractionation of REE appears only to depend on the amount of fluorine available for tephra dissolution. The same process is likely to explain the enrichment in other refractory elements observed at Hekla, and might also partly increase the apparent volatility of some volatile elements (e.g., Zr), provided they are both at significant concentration levels in magmas and mobile in F-rich fluids. This dissolution process is likely to have initiated and was the most efficient in the ascending sub-Plinian column at the moment of volatile species adsorption onto the tephra grains. It may have continued at a slower rate until snow samples were melted at the laboratory and filter to eliminate all tephra. This study shows that in addition to well-known volatile elements, significant amounts of refractory elements may be transported in F-rich volcanic plumes. Consequently, these elements may be readily mobilized and brought into terrestrial ecosystems upon thawing or at the first raining event. Tephra dissolution processes thus should be taken into account when estimating trace element mass balances during degassing processes and assessing the environmental impact and pollution and/or fertilization effects of volcanic activity.

Acknowledgments

We are much grateful to Gudrun Larsen and Armann Höskuldsson for supplying the tephra and lava samples for this study. Karine David and Gilles Chazot are acknowledged for their help with the analytical work. Discussions and help with thermodynamic calculations by Domenik Wolff-Boenisch were greatly appreciated. We thank P. Delmelle, D. Pyle, K. Suzuki, and M. Kusakabe for constructive reviews that led to significant improvements of the manuscript. We also acknowledge a grant from the Egide-Rannis Jules Verne program of the French–Icelandic scientific collaboration.

Associate editor: Minoru Kusakabe

Appendix A

Analytical results (in $\mu g\ g^{-1}$) for a duplicate of sample He27A and USGS reference material BHVO

Samples	He27A	He27A2	BHVO	BHVO[a]
Be	11.7	11.2	1.04	1.1 (0.3)
Co	60.0	63.4	47.3	45 (2)
Cu	161	158	131	136 (6)
Zn	909	1041	190	179 (5)
Rb	27.7	28.1	8.72	11 (2)
Sr	326	319	405	403 (25)
Y	18.2	16.8	26.4	27.6 (1.7)
Zr	1252	1137	184	179 (21)
Cd	98.6	95.6	0.040	0.069 (0.011)
Sb	0.617	0.648	0.139	0.159 (0.036)
Te	5.29	4.96	0.013	0.006 (0.002)
Ba	160	152	139	139 (14)
La	9.97	10.4	15.2	15.8 (1.3)
Ce	25.2	25.7	40.0	39.0 (4)
Pr	3.68	3.66	5.67	5.7 (0.4)
Nd	15.3	15.4	23.1	25.2 (2)
Sm	4.06	4.01	6.02	6.2 (0.3)
Eu	1.38	1.51	2.30	2.06 (0.08)
Gd	5.80	5.94	6.73	6.4 (0.5)
Tb	1.08	1.07	0.977	0.96 (0.08)
Dy	7.66	7.99	5.69	5.2 (0.3)
Ho	1.60	1.67	1.02	0.99 (0.08)
Er	4.61	4.62	2.67	2.4 (0.2)
Tm	0.655	0.720	0.341	0.330 (0.040)
Yb	4.18	4.27	1.94	2.02 (0.2)
Lu	0.587	0.587	0.278	0.291 (0.026)
Hf	30.2	28.8	4.54	4.38 (0.22)
Tl	11.2	11.1	0.051	0.058 (0.012)
Pb	21.1	19.3	2.08	2.6 (0.9)
Bi	0.253	0.239	0.012	0.018 (0.004)
Th	0.556	0.534	1.31	1.08 (0.15)
U	7.54	8.14	0.472	0.42 (0.06)

[a] Recommended values for BHVO reference material from Gladney and Roelandts (1988). Numbers in parentheses represent the acceptable standard deviation on recommended values.

References

Aiuppa, A., Dongarra, G., Valenza, M., 2003. Degassing of trace volatile metals during the 2001 eruption of Etna. In: Robock, A., Oppenheimer, C. (Eds.), *Volcanism and the Earth's Atmosphere*, *Geophys. Monograph*, vol. 139. Amer. Geophys. Union, Washington, DC, pp. 41–54.

Aiuppa, A., Federico, C., Giudice, G., Gurrieri, S., Paonita, A., Valenza, M., 2004. Plume chemistry provides insights into mechanisms of sulfur and halogen degassing in basaltic volcanoes. *Earth Planet. Sci. Lett.* **222**, 469–483.

Allard, P., Burton, M., Muré, F., 2005. Spectroscopic evidence for a lava fountain driven by previously accumulated magmatic gas. *Nature* **433**, 407–409.

Baldridge, W.S., McGetchin, T.R., Frey, F.A., 1973. Magmatic evolution of Hekla, Iceland. *Contrib. Mineral. Petrol.* **42**, 245–258.

Bilal, B.A., Langer, P., 1987. Complex formation of trace elements in geochemical systems: stability constants of fluoro complexes of the lanthanides in a fluorite bearing model system up to 200 °C and 1000 bar. *Inorg. Chim. Acta* **140**, 297–298.

Crowe, B.M., Finnegan, D.L., Zoller, W.H., Boyton, W.V., 1987. Trace element geochemistry of volcanic gases and particles from 1983–1984 eruptive episodes of Kilauea volcano. *J. Geophys. Res.* **92**, 13708–13714.

Delmelle, P., Stix, J., 2000. Volcanic gases. In: Sigurdsson, H.H., Houghton, B.F., McNutt, S.R., Rymer, H., Stix, J. (Eds.), *Encyclopedia of Volcanoes*. Academic Press, San Diego, pp. 803–815.

Delmelle, P., Villiéras, F., Pelletier, M., 2005. Surface area, porosity and water adsorption properties of fine volcanic ash particles. *Bull. Volcanol.* **67**, 160–169.

Frogner, P., Gislason, S.R., Óskarsson, N., 2001. Fertilizing potential of volcanic ash in ocean surface water. *Geology* **29**, 487–490.

Gauthier, P.J., Le Cloarec, M.F., 1998. Variability of alkali and heavy metal fluxes released by Mt. Etna volcano, Sicily, between 1991 and 1995. *J. Volcanol. Geotherm. Res.* **81**, 311–326.

Gauthier, P.J., Le Cloarec, M.F., Condomines, M., 2000. Degassing processes at Stromboli volcano inferred from short-lived disequilibria (^{210}Pb–^{210}Bi–^{210}Po. in volcanic gases. *J. Volcanol. Geotherm. Res.* **102**, 1–19.

Gemmell, J.B., 1987. Geochemistry of metallic trace elements in fumarolic condensates from Nicaraguan and Costa Rican volcanoes. *J. Volcanol. Geotherm. Res.* **33**, 131–181.

Gerlach, T.M., 1993. Oxygen buffering of Kilauea volcanic gases and the oxygen fugacity of Kilauea basalt. *Geochim. Cosmochim. Acta* **57**, 795–814.

Giggenbach, W.F., 1996. Chemical composition of volcanic gases. In: Scarpa, R., Tilling, R.I. (Eds.), *Monitoring and Mitigation of Volcano Hazards*. Springer-Verlag, Berlin, pp. 221–256.

Gislason, S.R., Arnorsson, S., Armannsson, H., 1996. Chemical weathering of basalt in southwest Iceland: effects of Runoff, age of rocks and vegetative/glacial cover. *Am. J. Sci.* **296**, 837–907.

Gislason, S.R., Oelkers, E.H., 2003. Mechanism, rates, and consequences of basaltic glass dissolution: II. An experimental study of the dissolution rates of basaltic glass as a function of pH and temperature. *Geochim. Cosmochim. Acta* **67**, 3817–3832.

Gladney, E.S., Roelandts, I., 1988. 1987 compilation of elemental concentration data for USGS BHVO-1, MAG-1, QLO-1, RGM-1, Sco-1, SDC-1, SGR-1 and STM-1. *Geostand. Newslett.* **14**, 253–362.

Goff, F., Janik, C.J., Delgado, H., Werner, C., Counce, D., Stimac, J., Siebe, C., Love, S.P., Williams, S.N., Fisher, T.P., Johsnson, L., 1998. Geochemical surveillance of magmatic volatiles at Popocatepetl Volcano, Mexico. *Geol. Soc. Am. Bull.* **110**, 695–710.

Greenland, L.P., 1987. Composition of gases from the 1984 eruption of Mauna Loa Volcano. In: Decker, R.W., Wright, T.L., Stauffer, P.H. (Eds.), *Volcanism in Hawaii*. U.S. Geological Survey Professional Paper, Report: P 1350, pp. 781–790.

Gudmundsson, A., Oskarsson, N., Gronvold, K., Saemundsson, K., Sigurdsson, O., Stefansson, R., Gislason, S.R., Einarsson, P., Brandsdottir, B., Larsen, G., Johannesson, H., Thordarson, T., 1992. The 1991 eruption of Hekla, Iceland. *Bull. Volcanol.* **54**, 238–246.

Haas, J.R., Shock, E.L., Sassani, D.C., 1995. Rare earth elements in hydrothermal systems: estimates of standard partial molal thermodynamic properties of aqueous complexes of the rare earth elements at high pressures and temperatures. *Geochim. Cosmochim. Acta* **59**, 4329–4350.

Hinkley, T.K., Le Cloarec, M.-F., Lambert, G., 1994. Fractionation of families of major, minor, and trace metals across the melt–vapor interface in volcanic exhalations. *Geochim. Cosmochim. Acta* **58**, 3255–3263.

Jaupart, C., 1996. Physical models of volcanic eruptions. *Chem. Geol.* **128**, 217–227.

Jaupart, C., 1998. Gas loss from magmas through conduit walls during eruption. In: Gilbert, J.S., Sparks, R.S.J. (Eds.), *The Physics of*

Explosive Volcanic Eruptions, vol. 145. Geol. Soc. Spec. Publ., pp. 73–90.

Lacasse, C., Karlsdottir, S., Larsen, G., Soosalu, H., Rose, W.I., Ernst, G.G.J., 2004. Weather radar observations of the Hekla 2000 eruption cloud, Iceland. *Bull. Volcanol.* **66**, 457–473.

Le Guern, F., 1988. *Ecoulements gazeux réactifs à hautes températures, mesures et modélisation*. Ph.D. thesis, Paris VII Univ.

Lewis, A.J., Palmer, M.R., Sturchio, N.C., Kemp, A.J., 1997. The rare earth element geochemistry of acid–sulphate and acid–sulphate–chloride geothermal systems from Yellowstone National Park, Wyoming, USA. *Geochim. Cosmochim. Acta* **61**, 695–706.

Lide, D.R., 1997. *CRC Handbook of Chemistry and Physics*, 78th ed. CRC Press, Boca Raton.

Luo, Y., Millero, F.J., 2004. Effects of temperature and ionic strength on the stabilities of the first and second fluoride complexes of yttrium and the rare earth elements. *Geochim. Cosmochim. Acta* **68**, 4301–4308.

Michard, A., Albarède, F., 1986. The REE content of some hydrothermal fluids. *Chem. Geol.* **55**, 51–60.

Michard, A., 1989. Rare earth element systematics in hydrothermal fluids. *Geochim. Cosmochim. Acta* **53**, 745–750.

Millero, F.J., 1992. Stability constants for the formation of rare earth inorganic complexes as a function of ionic strength. *Geochim. Cosmochim. Acta* **56**, 3123–3132.

Nriagu, J.O., 1989. A global assessment of natural sources of atmospheric trace metals. *Nature* **338**, 47–49.

Oelkers, E.H., Gislason, S.R., 2001. The mechanism, rates and consequences of basaltic glass dissolution: I. An experimental study of the dissolution rates of basaltic glass as a function of aqueous Al, Si and oxalic acid concentration at 25 °C and pH = 3 and 11. *Geochim. Cosmochim. Acta* **65**, 3671–3681.

Oskarsson, N., 1980. The interaction between volcanic gases and tephra: fluorine adhering to tephra of the 1970 Hekla eruption. *J. Volcanol. Geotherm. Res.* **8**, 251–266.

Oskarsson, N., 1981. The chemistry of Icelandic lava incrustations and the latest stages of degassing. *J. Volcanol. Geotherm. Res.* **10**, 93–111.

Parkhurst, D.L., Appelo, C.A.J., 1999. User's guide to PHREEQC (Version 2)—a computer program for speciation, batch-reaction, one-dimensional transport, and inverse geochemical calculations. *U.S.G.S. Water. Resour. Inv. Report* 99-4259.

Pennisi, M., Le Cloarec, M.F., Lambert, G., Le Roulley, J.C., 1988. Fractionation of metals in volcanic emissions. *Earth Planet. Sci. Lett.* **88**, 284–288.

Rampino, M.R., Self, S., 1992. Volcanic winter and accelerated glaciation following the Toba super-eruption. *Nature* **359**, 50–52.

Rose, W.I., Gu, Y., Watson, I.M., Yu, T., Bluth, G.J.S., Prata, A.J., Krueger, A.J., Krotkov, N., Carn, S., Fromm, M.D., Hunton, D.E., Ernst, G.G.J., Viggiano, A.A., Miller, J.M., Ballenthin, J.O., Reeves, J.M., Wilson, J.C., Anderson, B.E., Flittner, D.E., 2003. The February–March 2000 eruption of Hekla, Iceland from a satellite perspective. In: Robock, A., Oppenheimer, C. (Eds.), *Volcanism and the Earth's Atmosphere*, *Geophys. Monograph*, vol. 139. Amer. Geophys. Union, Washington, DC, pp. 107–132.

Rubin, K., 1997. Degassing of metals and metalloids from erupting seamount and mid-ocean ridge volcanoes: observations and predictions. *Geochim. Cosmochim. Acta* **61**, 3525–3542.

Sigmarsson, O., Condomines, M., Fourcade, S., 1992. A detailed Th, Sr and O isotope study of Hekla: differentiation processes in an Icelandic volcano. *Contrib. Mineral. Petrol.* **112**, 20–34.

Sigvaldasson, G.E., Oskarsson, N., 1986. Fluorine in basalts from Iceland. *Contrib. Mineral. Petrol.* **94**, 236–271.

Spadaro, F., Lefèvre, R.A., Ausset, P., 2002. Experimental rapid alteration of basaltic glass: implications for the origins of atmospheric particulates. *Geology* **30**, 671–674.

Symonds, R.B., Rose, W.I., Reed, M.H., Litchte, F.E., Finnegan, D.L., 1987. Volatilization, transport and sublimation of metallic and non-metallic elements in high temperature gases at Merapi Volcano, Indonesia. *Geochim. Cosmochim. Acta* **51**, 2083–2101.

Symonds, R.B., Rose, W.I., Bluth, G.J.S., Gerlach, T.M., 1994. Volcanic-gas studies: methods, results, and applications. In: Caroll, M.R., Holloway, J.R. (Eds.), *Rev. Mineral.*, vol. 30, Mineral. Soc. Am. pp. 1–66.

Taran, Y.A., Hedenquist, J.W., Korzhinsky, M.A., Tkachenko, S.I., Shmulovich, K.I., 1995. Geochemistry of magmatic gases from Kudryavy volcano, Iturup, Kuril Islands. *Geochim. Cosmochim. Acta* **59**, 1749–1761.

Textor, C., Graf, H.F., Herzog, M., 2003. Injection of gases into the stratosphere by explosive volcanic eruptions. J. Geophys. Res. 108-D19, ACH 5 1-17. doi:10.1029/2002JD002987.

Thorarinsson, S., Sigvaldasson, G.E., 1973. The Hekla eruption of 1970. *Bull. Volcanol.* **36**, 269–288.

Thordarson, T., Self, S., Oskarsson, N., Hulsebosh, T., 1996. Sulfur, chlorine and fluorine degassing and atmospheric loading by the 1783–1784 AD Laki (Skaftar Fires) eruption in Iceland. *Bull. Volcanol.* **58**, 205–225.

Thordarson, T., Miller, D.J., Larsen, G., Self, S., Sigurdsson, H., 2001. New estimates of sulfur degassing and atmospheric mass-loading by the 934 AD Eldgjà eruption, Iceland. *J. Volcanol. Geotherm. Res.* **108**, 33–54.

Toutain, J.P., Sortino, F., Reynier, B., Dupré, B., Munoz, M., Nonell, A., Polve, M., Chancha Do Vale, S., 2003. A new collector for sampling volcanic aerosols. *J. Volcanol. Geotherm. Res.* **123**, 95–103.

White, A.F., Hochella Jr., M.F., 1992. Surface chemistry associated with the cooling and subaerial weathering of recent basalt flows. *Geochim. Cosmochim. Acta* **56**, 3711–3721.

Witham, C.S., Oppenheimer, C., Horwell, C.J., 2005. Volcanic ash-leachates: a review and recommendations for sampling methods. *J. Volcanol. Geotherm. Res.* **141**, 299–326.

Withby, K.T., 1978. The physical characteristics of sulfur aerosols. *Atmos. Environ.* **12**, 135–139.

Wolff-Boenisch, D., Gislason, S.R., Oelkers, E.H., 2004a. The effect of fluoride on the dissolution rates of natural glasses at pH 4 and 25 °C. *Geochim. Cosmochim. Acta* **68**, 4571–4582.

Wolff-Boenisch, D., Gislason, S.R., Oelkers, E.H., Putnis, C.V., 2004b. The dissolution of natural glasses as a function of the composition at pH 4 and 10.6, and temperature from 25 to 74 °C. *Geochim. Cosmochim. Acta* **68**, 4843–4858.

Wood, S.A., 1990a. The aqueous geochemistry of the rare-earth elements and yttrium 1—review of available low-temperature data for inorganic complexes and the inorganic REE speciation of natural waters. *Chem. Geol.* **82**, 159–186.

Wood, S.A., 1990b. The aqueous geochemistry of the rare-earth elements and yttrium 2—theoretical predictions of speciation in hydrothermal solutions to 350 °C at saturation water vapor pressure. *Chem. Geol.* **88**, 99–125.

Zoller, W.H., Gladney, E.S., Duce, R.A., 1974. Atmospheric concentrations and sources of trace metals at the South Pole. *Science* **183**, 198–200.